The link between volcanism and plutonism in epizonal magma systems; high-precision U–Pb zircon geochronology from the Organ Mountains caldera and batholith, New Mexico

Contrib Mineral Petrol (2016) 171:13
DOI 10.1007/s00410-015-1208-6

ORIGINAL PAPER

The link between volcanism and plutonism in epizonal magma systems; high-precision U–Pb zircon geochronology from the Organ Mountains caldera and batholith, New Mexico

Matthew Rioux[1,2] · G. Lang Farmer[3] · Samuel A. Bowring[2] · Kathleen M. Wooton[4] · Jeffrey M. Amato[5] · Drew S. Coleman[4] · Philip L. Verplanck[6]

Received: 1 June 2015 / Accepted: 12 November 2015 / Published online: 21 January 2016

Abstract The Organ Mountains caldera and batholith expose the volcanic and epizonal plutonic record of an Eocene caldera complex. The caldera and batholith are well exposed, and extensive previous mapping and geochemical analyses have suggested a clear link between the volcanic and plutonic sections, making this an ideal location to study magmatic processes associated with caldera volcanism. Here we present high-precision thermal ionization mass spectrometry U–Pb zircon dates from throughout the caldera and batholith, and use these dates to test and improve existing petrogenetic models. The new dates indicate that Eocene volcanic and plutonic rocks in the Organ Mountains formed from ~44 to 34 Ma. The three largest caldera-related tuff units yielded weighted mean $^{206}Pb/^{238}U$ dates of 36.441 ± 0.020 Ma (Cueva Tuff), 36.259 ± 0.016 Ma (Achenback Park tuff), and 36.215 ± 0.016 Ma (Squaw Mountain tuff). An alkali feldspar granite, which is chemically similar to the erupted tuffs, yielded a synchronous weighted mean $^{206}Pb/^{238}U$ date of 36.259 ± 0.021 Ma. Weighted mean $^{206}Pb/^{238}U$ dates from the larger volume syenitic phase of the underlying Organ Needle pluton range from 36.130 ± 0.031 to 36.071 ± 0.012 Ma, and the youngest sample is 144 ± 20 to 188 ± 20 ka younger than the Squaw Mountain and Achenback Park tuffs, respectively. Younger plutonism in the batholith continued through at least 34.051 ± 0.029 Ma. We propose that the Achenback Park tuff, Squaw Mountain tuff, alkali feldspar granite and Organ Needle pluton formed from a single, long-lived magma chamber/mush zone. Early silicic magmas generated by partial melting of the lower crust rose to form an epizonal magma chamber. Underplating of the resulting mush zone led to partial melting and generation of a high-silica alkali feldspar granite cap, which erupted to form the tuffs. The deeper parts of the chamber underwent continued recharge and crystallization for 144 ± 20 ka after the final eruption. Calculated magmatic fluxes for the Organ Needle pluton range from 0.0006 to 0.0030 km^3/year, in agreement with estimates from other well-studied plutons. The petrogenetic evolution proposed here may be common to many small-volume silicic volcanic systems.

Keywords Organ Mountains · Tuff · Epizonal · Zircon · Pluton · Organ Needle pluton · Caldera

Communicated by Timothy L. Grove.

Electronic supplementary material The online version of this article (doi:10.1007/s00410-015-1208-6) contains supplementary material, which is available to authorized users.

✉ Matthew Rioux
rioux@eri.ucsb.edu

[1] Earth Research Institute, University of California, Santa Barbara, Santa Barbara, CA 93106, USA

[2] Department of Earth, Atmospheric and Planetary Sciences, Massachusetts Institute of Technology, Cambridge, MA 02459, USA

[3] Department of Geological Sciences, University of Colorado, Boulder, CO 80309, USA

[4] Department of Geological Sciences, University of North Carolina, Chapel Hill, NC 27599, USA

[5] Department of Geological Sciences, New Mexico State University, Las Cruces, NM 88003, USA

[6] U.S. Geological Survey, Denver, CO 80225, USA

Introduction

Large silicic caldera eruptions can have regional to global impacts. To fully understand caldera magmatism, and

ultimately the potential hazards posed by these systems, it is necessary to understand the link between intrusive and extrusive magmatism. The role of shallow (<8 km depth) plutons has been debated. Many studies have argued that silicic tuffs undergo fractionation in the upper- to mid-crust prior to eruption and that plutons represent the residual solids from this processes (e.g., Bachmann and Bergantz 2004, 2008; Bachmann et al. 2007; Hildreth 1981, 2004; Lipman 1984, 2007; Lipman and Bachmann 2015; Metcalf 2004; Smith 1979). On the other hand, two recent geochronologic studies have documented an offset between the timing of caldera-related volcanic eruptions and crystallization of spatially associated shallow plutons (Mills and Coleman 2013; Tappa et al. 2011) . These and earlier studies have suggested that the relative role of volcanism and plutonism may be related to magmatic fluxes, where high flux regimes favor eruption of silicic magmas formed lower in the crust and lower flux regimes favor intrusive crystallization (Glazner et al. 2004; Mills and Coleman 2013; Tappa et al. 2011).

The Eocene Organ Mountains caldera and batholith, south-central New Mexico, are ideal places to study the link between silicic volcanism and epizonal plutonism in a small- to intermediate-volume system. The batholith is exposed directly below preserved caldera deposits, and field relationships and geochemical differentiation trends suggest a genetic link between the plutonic and volcanic sections. Previous studies have used detailed mapping and geochemical analyses to develop petrogenetic models for the system (Seager 1981; Seager and McCurry 1988; Verplanck et al. 1995, 1999). These studies demonstrated geochemical zoning within the plutonic section, which was attributed to magmatic differentiation prior to and during eruption of the caldera tuffs. The zoning is consistent with chemical zonation observed in large silicic eruptions (Bachmann and Bergantz 2008; Hildreth 1981). The proposed petrogenetic models can be further tested using high-precision geochronology; however, prior to the present study, the timing of pluton crystallization in the Organ Mountains batholith was poorly constrained (Zimmerer and McIntosh 2013). Here, we present new high-precision isotope dilution-thermal ionization mass spectrometry (ID-TIMS) U–Pb zircon geochronology and whole-rock radiogenic isotope data from both the volcanic and plutonic sections in the Organ Mountains. Our new data provide insight into the link between volcanism and epizonal plutonism, constrain magmatic fluxes, constrain the lifespan of upper crustal magma chambers/mush zones, and directly test and improve existing petrogenetic models for this well-studied system.

Geologic setting

Eocene magmatism in southern New Mexico is generally attributed to the end of the Laramide subduction event and subsequent Rio Grande rift extension. Laramide subduction in New Mexico was accompanied by magmatism at 75 Ma and 48 to 37 Ma (e.g., McMillan 2004). The younger phase of magmatism is marked by intermediate (primarily andesite) composite cones with extensive lava flows and lahars. A change in eruptive composition and style, to large rhyolitic caldera complexes, occurred at ~37 Ma and is attributed to the early phase of Rio Grande rift extension (Cather et al. 1984; Mack et al. 1998; McMillan et al. 2000). The Organ Mountains caldera and batholith likely formed as a result of the early rift magmatism (Seager and McCurry 1988).

The Organ Mountains caldera and batholith were intruded into and erupted onto Proterozoic granite and Paleozoic sedimentary rocks (Fig. 1). The preserved volcanic stratigraphy consists of the Orejon Andesite (0.5–1 km), Cueva Tuff (0.2–0.6 km), Achenback Park tuff (informally named; 0.2–1 km), Squaw Mountain tuff (informally named; 0.7–1.4 km) and West-side lavas (Fig. 1) (Seager 1981; Seager and McCurry 1988). The Orejon Andesite includes intermediate composition flows and lahar breccias and has been interpreted to represent preexisting volcanic cover or early eruptions related to the caldera-forming magmatism (Seager and McCurry 1988). The Cueva Tuff is the oldest of the caldera-forming ignimbrites and consists of numerous variably welded rhyolitic ash-flow tuffs. The overlying Achenback Park and Squaw Mountain tuffs are each composed of a single cooling unit of moderate to densely welded rhyolitic ash-flow tuff. The West-side lavas are the youngest eruptive unit and include rhyolite, trachyte and dacite lava flows (unit descriptions based on Seager and McCurry 1988). The ash-flow tuff units are separated by disconformities marked by volcaniclastic sandstones and breccias. The estimated total erupted volume is 300–1000 km^3 (Seager and McCurry 1988; Verplanck et al. 1999).

The Organ Mountains batholith, located directly below and intruding into the Orejon Andesite and Cueva Tuff, is composed of the Organ Needle pluton, the granite of Granite Peak and the Sugarloaf Peak quartz monzonite. The Organ Needle pluton (ONP) is the largest intrusive unit and includes phases of equigranular syenite/quartz syenite (EQS), inequigranular syenite/quartz syenite (IEQ), monzodiorite and alkali feldspar granite (AFG) (Seager 1981; Seager and McCurry 1988; Verplanck et al. 1995, 1999). The inequigranular syenite is exposed in a thin zone at the lowest structural levels of the pluton (Verplanck et al. 1995, 1999). The syenitic phases of the pluton are chemically stratified from more mafic compositions at the base to more silicic compositions at higher structural levels. The alkali feldspar granites form three cupolas at the highest structural levels and intruded into the Orejon Andesite and Cueva Tuff (Fig. 1). The granite of Granite Peak intruded

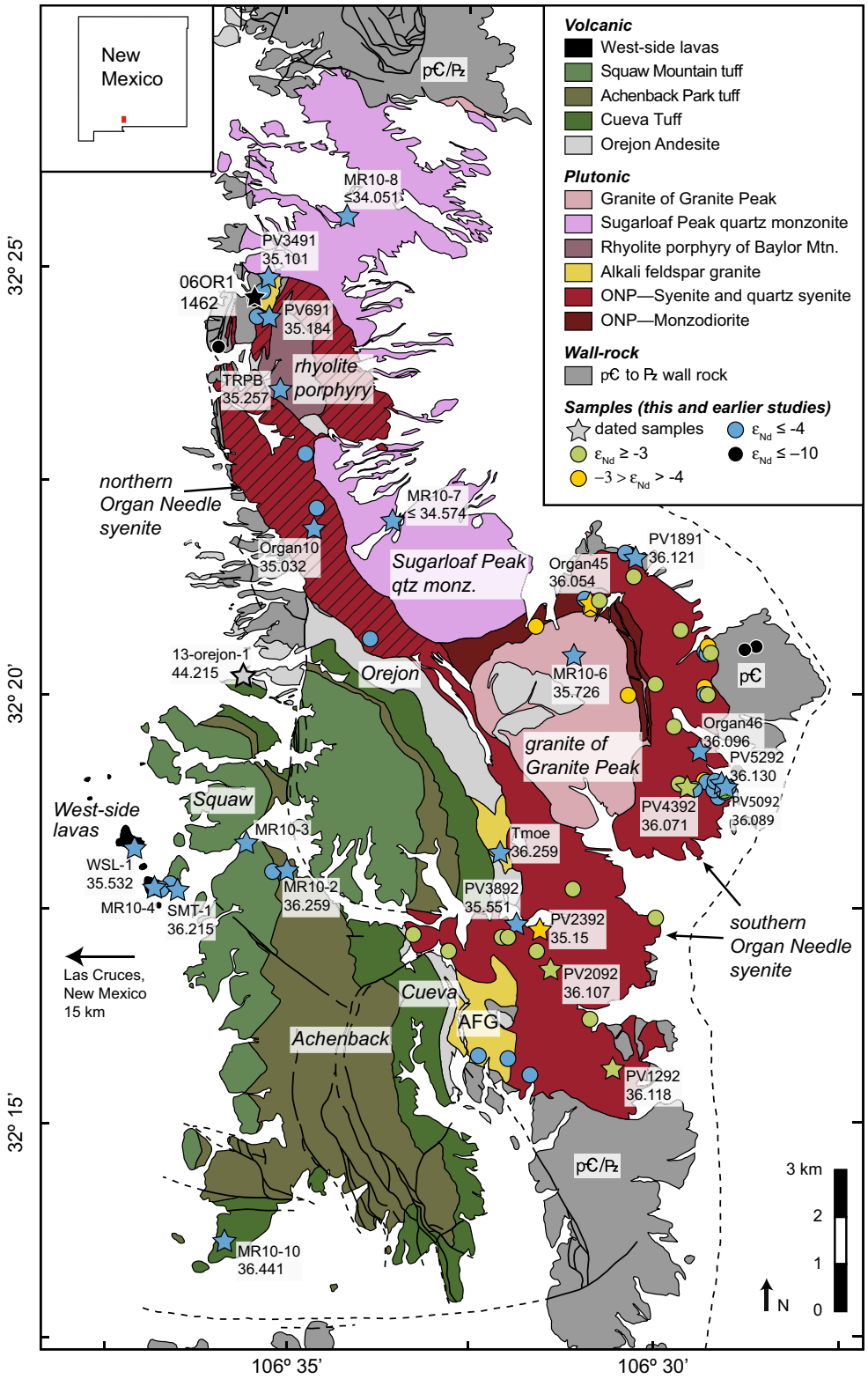

Fig. 1 Geologic map of the Organ Mountains (after Seager 1981; Verplanck et al. 1999). Location map inset in the upper left. *Stars* denote locations of samples analyzed in this study. *Circles* denote sample locations from Verplanck et al. (1995, 1999) and Butcher (1990). Sample labels include sample numbers and dates in Ma, based on the data presented in this manuscript. The hatched pattern denotes the northern exposures of mapped Organ Needle pluton syenites, which our U–Pb dates indicate are significantly younger than the main southern portion of the pluton. Sample symbols are color-coded based on whole-rock ε_{Nd}, as outlined in the key. ONP, Organ Needle pluton; AFG, alkali feldspar granite. The isotopic compositions of samples Organ10, Organ45, Organ46, 06OR1, WSL-1, SMT-1, and Tmoe are inferred from other analyzed samples from the same unit

into the center of the Organ Needle pluton. The Sugarloaf Peak quartz monzonite includes monzonitic to granitic compositions and intruded along the northeastern side of the Organ Needle pluton.

Existing geochemistry and petrogenetic models

Seager and McCurry (1988) argued that the ignimbrites and lavas of the Organ Mountains caldera, including the Cueva Tuff, Achenback Park tuff, Squaw Mountain tuff and West-side lavas, were formed by repeated eruptions from a single, chemically stratified magma chamber. This interpretation was based on the minimal erosion between the eruptive units and the relatively smooth chemical trends from the bottom to the top of the volcanic series: SiO_2 decreases from the Cueva Tuff (72–76 wt%) through the West-side lavas (61–66 wt%), while TiO_2, Al_2O_3, FeO*, MgO, and CaO increase. The authors argued that the chemical trends are consistent with eruptions sourced from progressively deeper in the silica-rich cap of a stratified magma chamber, with the Organ Needle pluton representing the preserved remnants of deeper levels in the magma chamber.

Verplanck et al. (1995, 1999) used field relationships, petrography, and whole-rock and mineral chemical and isotopic analyses to develop a more detailed model for the formation of the Organ Needle pluton. These and earlier studies showed that the Organ Needle pluton is compositionally stratified from more mafic compositions at the base (~57 wt% SiO_2) to more felsic compositions at the top (68–76 wt% SiO_2) (Seager and McCurry 1988; Verplanck et al. 1995, 1999). The data in Verplanck et al. (1995, 1999) further demonstrated isotopic zoning within the pluton; the equigranular syenite at the center of the pluton has $\varepsilon_{Nd}(t) \approx -2$, while the inequigranular syenite at the base of the pluton and the alkali feldspar granite cupolas at the top of the pluton have $\varepsilon_{Nd}(t) \approx -5$. A thin channel (20–100 m) of rocks that have $\varepsilon_{Nd}(t) \approx -5$ and are more silicic than adjacent equigranular syenite is also preserved along the margin of the Organ Needle pluton at higher structural levels; Fig. 1 shows the distribution of isotopic data from the present study, Verplanck et al. (1995, 1999) and Butcher (1990). The Proterozoic wall rocks of the pluton have $\varepsilon_{Nd}(t) \approx -12$ (Verplanck et al. 1995, 1999). Based on the isotopic data, geochemical data and field relations, Verplanck et al. (1995, 1999) suggested that the $\varepsilon_{Nd}(t) \approx -5$ magmas in the pluton were likely generated by assimilation of $\varepsilon_{Nd}(t) \approx -12$ wall rock into the $\varepsilon_{Nd}(t) \approx -2$ magma that formed the core of the pluton. The absence of a correlation between Nd concentrations and $\varepsilon_{Nd}(t)$ for the $\varepsilon_{Nd}(t) \approx -5$ rocks was interpreted to indicate that wall rock assimilation occurred at depth, followed by differentiation and migration of the resultant magma (Verplanck et al. 1995, 1999).

Based on the observations outlined above, Verplanck et al. (1995, 1999) developed a four-stage model for the evolution of the Organ Needle pluton and eruption of the Squaw Mountain tuff (Fig. 14 of Verplanck et al. 1999): (1) An $\varepsilon_{Nd}(t) \approx -2$ magma intruded into the Proterozoic wall rocks. (2) Partial melting and assimilation of the wall rocks at the base of the pluton generated an $\varepsilon_{Nd}(t) \approx -5$ magma. (3) The $\varepsilon_{Nd}(t) \approx -5$ magma underwent differentiation and migrated upwards along the sides of the pluton, encapsulating the shallower $\varepsilon_{Nd}(t) \approx -2$ magma. The encapsulated magma also underwent differentiation, leading to the observed compositional stratification. (4) The $\varepsilon_{Nd}(t) \approx -5$ magma that reached the shallowest depths erupted to form the Squaw Mountain tuff. The intrusive equivalents crystallized to form the alkali feldspar granite cupolas.

A major goal of the present study was to use high-precision geochronology to test and improve the Verplanck et al. (1995, 1999) model. The samples we dated include both samples analyzed for geochemical and isotopic compositions in these previous studies and a suite of samples we collected to augment the existing sample suite.

Existing geochronology

Existing geochronology from the Organ Mountains caldera and batholith includes K–Ar, $^{40}Ar/^{39}Ar$ and laser ablation-inductively coupled plasma-mass spectrometry (LA–ICP–MS) U–Pb dates. Loring and Loring (1980), Seager (1981), McIntosh et al. (1990) and Verplanck et al. (1995) reported limited K–Ar and $^{40}Ar/^{39}Ar$ dates from the volcanic and plutonic sections. In a recent, larger study, Zimmerer and McIntosh (2013) acquired $^{40}Ar/^{39}Ar$ sanidine, K-feldspar, biotite and hornblende dates from plutonic and volcanic rocks throughout the Organ Mountains (Supplementary Figure SM1). Weighted mean $^{40}Ar/^{39}Ar$ sanidine dates for the Cueva Tuff, Achenback Park tuff, and Squaw Mountain tuff were 36.45 ± 0.08, 36.23 ± 0.14, and 36.03 ± 0.16 Ma, respectively (uncertainties throughout are ±2σ internal). $^{40}Ar/^{39}Ar$ sanidine, biotite, hornblende, plagioclase and groundmass dates from the younger West-side lavas ranged from 36.28 ± 0.23 to 35.68 ± 0.09 Ma. Finally, $^{40}Ar/^{39}Ar$ biotite cooling and/or reheating dates from the different components of the Organ Needle pluton, the granite of Granite Peak and the Sugarloaf Peak quartz monzonite ranged from 36.25 ± 0.12 to 33.46 ± 0.19 Ma. Zimmerer and McIntosh (2013) also reported a smaller number of laser ablation-inductively coupled plasma-mass spectrometry (LA–ICP–MS) U–Pb zircon dates from the Organ Mountains batholith, but the utility of the data is limited by relatively large analytical uncertainties (±0.4–0.9 Ma). The best estimate of the age of the Orejon Andesite comes from $^{40}Ar/^{39}Ar$ hornblende and biotite dates of 46–40 Ma from

the correlative Rubio Peak Formation, exposed in adjacent ranges in south-central New Mexico (McMillan 2004).

The existing radiometric dates precisely date the volcanic units, but place only limited constraints on the age of pluton crystallization; the LA–ICP–MS U–Pb dates have large uncertainties, and the $^{40}Ar/^{39}Ar$ dates provide cooling or reheating dates for the plutonic rocks. Here, we build on these previous studies using high-precision U–Pb zircon geochronology, which provides a detailed record of the timing of plutonism and volcanism in the Organ Mountains.

Terminology

For clarity and brevity in this manuscript, we will adopt a simplified terminology for the different units of the Organ Mountains caldera and batholith based on the combined mineralogy, textures, and isotopic composition. The Organ Needle pluton will be used to refer to the syenite to quartz syenite and monzodioritic rocks from the central Organ Mountains, excluding the alkali feldspar cupolas that are in contact with these units. Within the pluton, we refer to syenitic to quartz syenitic rocks from the center of the pluton, which have $\varepsilon_{Nd}(t) \approx -2$, as "equigranular syenites." We will refer to inequigranular syenitic to quartz syenitic rocks from the base of the pluton, which have $\varepsilon_{Nd}(t) \approx -5$, as "inequigranular syenites." Additional $\varepsilon_{Nd}(t) \approx -5$ syenitic rocks are also located along the margins of the equigranular syenite at higher structural levels but do not have inequigranular textures. The new U–Pb dates presented herein suggest that the northern arm of the equigranular Organ Needle syenites (marked with a hatched pattern in Fig. 1) is significantly younger than the main southeastern syenite body, and we will therefore differentiate between the northern and southern Organ Needle syenites (Fig. 1). Similarly, we differentiate between the northern alkali feldspar granite cupola (northern AFG) and central and southern alkali feldspar granite cupolas (southern AFG). Finally, we will abbreviate the tuff of Squaw Mountain and the tuff of Achenback Park as the Squaw Mountain tuff and Achenback Park tuff, and refer to the lavas overlying the Squaw Mountain tuff as the West-side lavas.

Results

Our new U–Pb dates from the Eocene caldera and batholith are presented in Figs. 1, 2, 3, and 4, and in Supplementary Tables SM1 and SM2. Twenty samples were dated in the Radiogenic Isotope Laboratory at the Massachusetts Institute of Technology (MIT; Supplementary Table SM1), and three additional samples were dated in the Geochronology and Isotope Geochemistry Laboratory at the University of North Carolina (UNC; Supplementary Table SM2). Analytical methods, including a detailed discussion of the Th correction applied to the zircon $^{206}Pb/^{238}U$ dates, are provided in the Supplementary Text and Supplementary Figure SM2; all $^{206}Pb/^{238}U$ dates in the text and figures are Th-corrected. A single sample of Paleozoic wall rock was dated using the sensitive high resolution ion microprobe-reverse geometry (SHRIMP-RG) at Stanford University (Supplementary Text, Supplementary Table SM3, and Supplementary Figure SM3). Sample locations are provided in Table 1.

For the volcanic and plutonic samples in this study, high-precision $^{206}Pb/^{238}U$ dates from a subset of samples define a single population (mean square of the weighted deviates of the weighted mean; MSWD $\approx$ 1), but most samples contain a range of dates with a MSWD that is higher than expected for a single population (two-sided p value for the Chi-square goodness of fit $\leq$0.05; MSWD $\geq$ 2–3, depending on n). The scatter in dates for most samples could be explained by Pb loss, inheritance or protracted zircon growth in a magma (magma residence). We applied the chemical abrasion method to all of the dated zircons, which minimizes or eliminates the effects of Pb loss in most grains (Mattinson 2005), making it unlikely that there is widespread Pb loss. In most cases, we therefore interpret the intra-sample variations in dates to reflect either magma residence times or assimilation of zircons from older rocks related to the same magmatic system. Interestingly, we only observed older zircons that could reflect inheritance of xenocrysts from the Proterozoic wall rocks in a single sample (Organ10), suggesting that any assimilated grains were efficiently dissolved in the magmas. In the cases of magma residence or inheritance, the youngest date or population of dates in each sample provides the best estimate for the eruption age or final crystallization age of the rock. We calculated weighted mean dates for the youngest population in each sample and interpret these to be the best estimate of the crystallization or eruption age of the sample; however, we note that if we instead take only the youngest date in each sample as the crystallization or eruption age, it does not change the conclusions reached herein. Detailed results for each sample are discussed by map unit below.

Proterozoic granite wall rock

SHRIMP data from a single sample yielded concordant and variably discordant data that plot along a discordia line with an upper intercept of 1452 $+33/-26$ Ma (MSWD $= 2.1$, $n = 8$, Supplementary Table SM3, Supplementary Figure SM3). The lower intercept yielded a poorly constrained date of 91 $\pm$ 170 Ma. The three most concordant spot analyses yielded a weighted mean $^{207}Pb/^{206}Pb$ date of 1462 $\pm$ 28 Ma (MSWD $= 2.1$, $n = 3$), within uncertainty of the calculated upper intercept date. We interpret the weighted mean date of

the three most concordant points to be the best estimate of the crystallization age of the Proterozoic granite.

Volcanic rocks

The dated volcanic samples come from each of the major volcanic units: the Orejon Andesite, Cueva Tuff, Achenback Park tuff, Squaw Mountain tuff, and West-side lavas. Dated zircons from the Squaw Mountain tuff and West-side lavas define single populations with weighted mean $^{206}Pb/^{238}U$ dates of 36.215 ± 0.016 Ma (SMT-1, MSWD = 0.96, $n = 6/6$; ratio denotes number of fractions/zircons included in the weighted mean over the number of fractions/zircons analyzed) and 35.532 ± 0.030 (WSL-1, MSWD = 0.40, $n = 5/5$), respectively. For the remaining volcanic samples, interpreted weighted mean $^{206}Pb/^{238}U$ dates or single-grain dates for each sample were as follows: Orejon Andesite, 44.215 ± 0.054 Ma (13-orejon-1, iz12, $n = 1/4$); Cueva Tuff, 36.441 ± 0.020 Ma (MR10-10, MSWD = 2.2, $n = 2/9$); and Achenback Park tuff, 36.259 ± 0.016 Ma (MR10-2, MSWD = 1.7, $n = 6/7$) (Figs. 2, 4).

One concern in using U–Pb zircon geochronology to date volcanic eruptions is the possibility that zircons may have crystallized in a magma tens to hundreds of thousands of years prior to eruption (magma residence time) (e.g., Simon et al. 2008). Comparison of the U–Pb dates reported here and published $^{40}Ar/^{39}Ar$ dates (Zimmerer and McIntosh 2013) (Supplementary Figure SM1) suggest that this was not a major issue in this study. Zimmerer and McIntosh (2013) used the recalibrated age of the Fish Canyon Tuff standard (Kuiper et al. 2008) and revised estimates of the ^{40}K decay constant (Min et al. 2000), which minimize biases between the U–Pb and K–Ar systems. The Zimmerer and McIntosh (2013) $^{40}Ar/^{39}Ar$ dates overlap our weighted mean $^{206}Pb/^{238}U$ dates for the Cueva Tuff, Achenback Park tuff and Squaw Mountain tuff, within uncertainty, consistent with minimal residence time for the dated zircons prior to eruption. $^{40}Ar/^{39}Ar$ dates for the West-side lavas are older than our U–Pb dates and may be inaccurate. In the present study, we rely on the U–Pb zircon dates for the volcanic units, in order to ensure that the data are internally consistent with the dates from the plutonic section.

Organ Needle pluton and alkali feldspar granites

Organ Needle pluton syenite

Seven dated samples from mapped exposures of the equigranular and inequigranular syenite yielded similar dates, while four other samples were significantly younger. Three samples from the equigranular syenite with $\varepsilon_{Nd}(t) \approx -2$ yielded interpreted weighted mean $^{206}Pb/^{238}U$ dates of 36.118 ± 0.017 Ma (PV1292, MSWD = 0.066, $n = 4/6$); 36.107 ± 0.016 Ma (PV2092, MSWD = 1.4, $n = 6/7$); and 36.071 ± 0.012 Ma (PV4392, MSWD = 0.12, $n = 4/6$). Two samples from the basal inequigranular syenite and a single sample from a higher border syenite, which all have $\varepsilon_{Nd}(t) \approx -5$, yielded interpreted weighted mean $^{206}Pb/^{238}U$ dates of 36.121 ± 0.016 Ma (PV1891, MSWD = 1.5, $n = 4/6$); 36.089 ± 0.017 Ma (PV5092, MSWD = 0.36, $n = 3/8$); and 36.130 ± 0.031 Ma (PV5292, IEQ, MSWD = 1.7, $n = 3/6$). A final sample of inequigranular syenite, which does not have Nd or Sr isotopic data, yielded a synchronous interpreted weighted mean $^{206}Pb/^{238}U$ date of 36.096 ± 0.047 Ma (Organ46, MSWD = 0.89, $n = 2/5$). For PV4392, we excluded one younger date and one older date and took the weighted mean of four zircons with nearly identical $^{206}Pb/^{238}U$ dates; the one slightly younger date is anomalously young compared to other analyses from both this sample and the six other samples described above and may reflect residual Pb loss that was not removed by the chemical abrasion method. The seven dated samples are distributed throughout the syenitic phase of the pluton and include both equigranular and inequigranular rocks, and we interpret the dates to reflect the crystallization age of the main southern phase of the Organ Needle pluton.

Four samples from the northern exposure of the syenite, exposed west of the Sugarloaf Peak quartz monzonite (marked with a hatched pattern in Fig. 1), and from two exposures in the middle of the southern lobe of the syenite yielded significantly younger dates. The two samples of equigranular syenite from the northern arm of the syenite yielded weighted mean $^{206}Pb/^{238}U$ dates of 35.184 ± 0.020 Ma (PV691, MSWD = 1.2, $n = 5/6$) and 35.032 ± 0.070 Ma (Organ10, MSWD = 1.8, $n = 3/11$). Sample Organ10 contains two older fractions; one fraction was concordant with a $^{206}Pb/^{238}U$ date of 79.53 ± 0.35, and the second fraction was discordant with a $^{206}Pb/^{238}U$ date of 88.4 ± 1.1 Ma.

Fig. 2 Wetherill U–Pb concordia diagrams and weighted mean $^{206}Pb/^{238}U$ plots for samples dated at the Massachusetts Institute of Technology. Each data point is an analysis of a single zircon or zircon fragment. All data are corrected for initial ^{230}Th exclusion, as discussed in the Supplementary Text. Ages on concordia are in Ma. Gray bands represent 2σ uncertainties on concordia based on decay constant uncertainties of 0.107 % (^{238}U) and 0.136 % (^{235}U) (Jaffey et al. 1971). Axis labels are shown in the upper left plot on each page. Gray data points are included in the weighted mean calculation. For the weighted mean plots, the reported date is either the weighted mean date (Ma) or, for complex samples, the youngest zircon date, which we interpret as a maximum crystallization age (labeled as youngest date). Plots and mean square of the weighted deviates (MSWD) of the weighted mean (wtd. mn.) were generated using the ET_Redux software package (Bowring et al. 2011; McLean et al. 2011). EQS-S, southern equigranular syenite; IEQ-S, southern inequigranular syenite; EQS-N, northern equigranular syenite; MZD, Organ Needle monzodiorite; AFG-N, northern alkali feldspar granite; AFG-S, middle and southern alkali feldspar granites; RPB, rhyolite porphyry of Baylor Mountain; GPK, granite of Granite Peak; SPQM, Sugarloaf Peak quartz monzonite; SMT, Squaw Mountain tuff; APT, Achenback Park tuff; Cueva, Cueva Tuff; WSL, West-side lavas

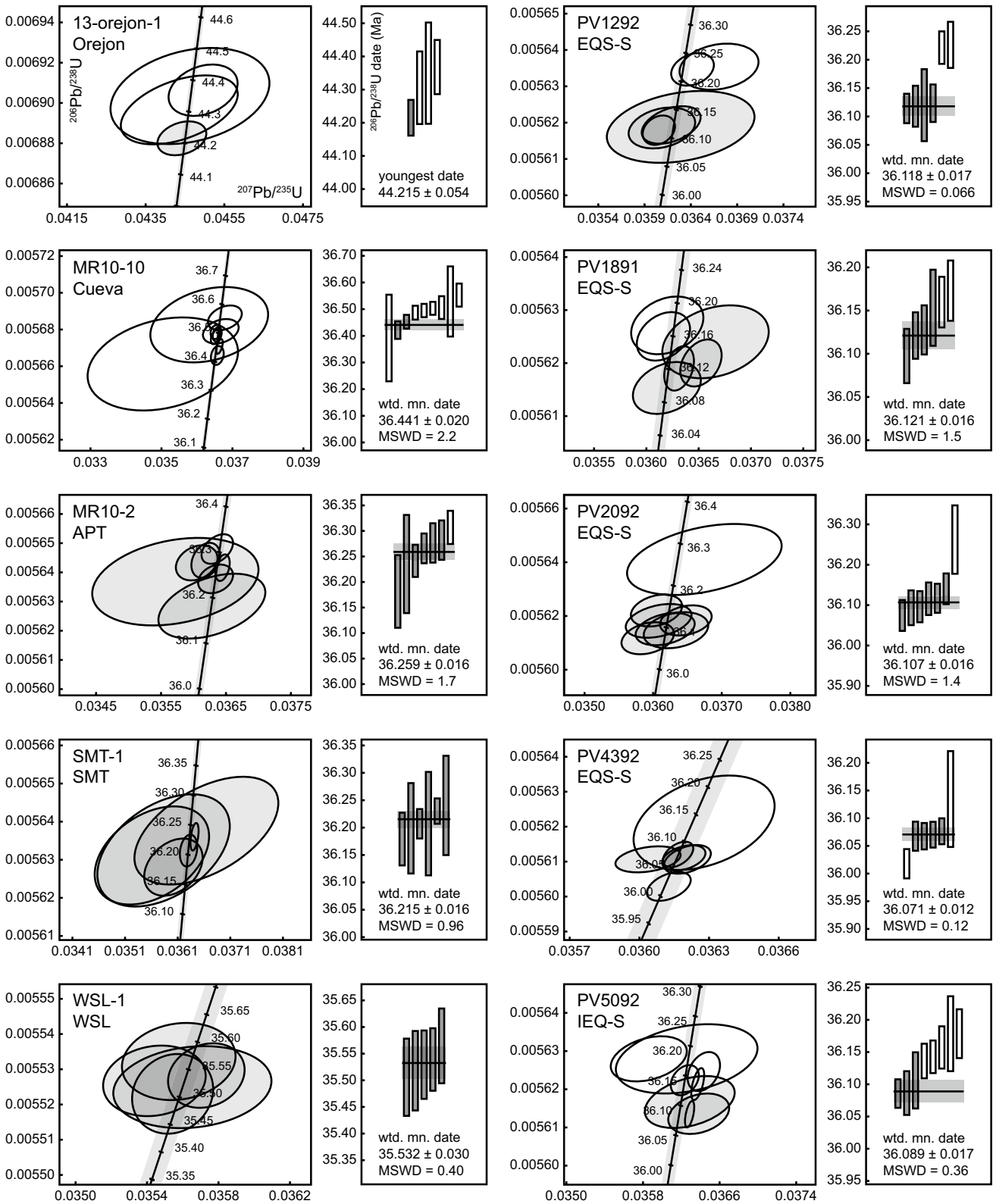
Volcanic
Plutonic
13-orejon-1
Orejon
youngest date
44.215 ± 0.054
MR10-10
Cueva
wtd. mn. date
36.441 ± 0.020
MSWD = 2.2
MR10-2
APT
wtd. mn. date
36.259 ± 0.016
MSWD = 1.7
SMT-1
SMT
wtd. mn. date
36.215 ± 0.016
MSWD = 0.96
WSL-1
WSL
wtd. mn. date
35.532 ± 0.030
MSWD = 0.40
PV1292
EQS-S
wtd. mn. date
36.118 ± 0.017
MSWD = 0.066
PV1891
EQS-S
wtd. mn. date
36.121 ± 0.016
MSWD = 1.5
PV2092
EQS-S
wtd. mn. date
36.107 ± 0.016
MSWD = 1.4
PV4392
EQS-S
wtd. mn. date
36.071 ± 0.012
MSWD = 0.12
PV5092
IEQ-S
wtd. mn. date
36.089 ± 0.017
MSWD = 0.36
206Pb/238U
207Pb/235U
206Pb/238U date (Ma)

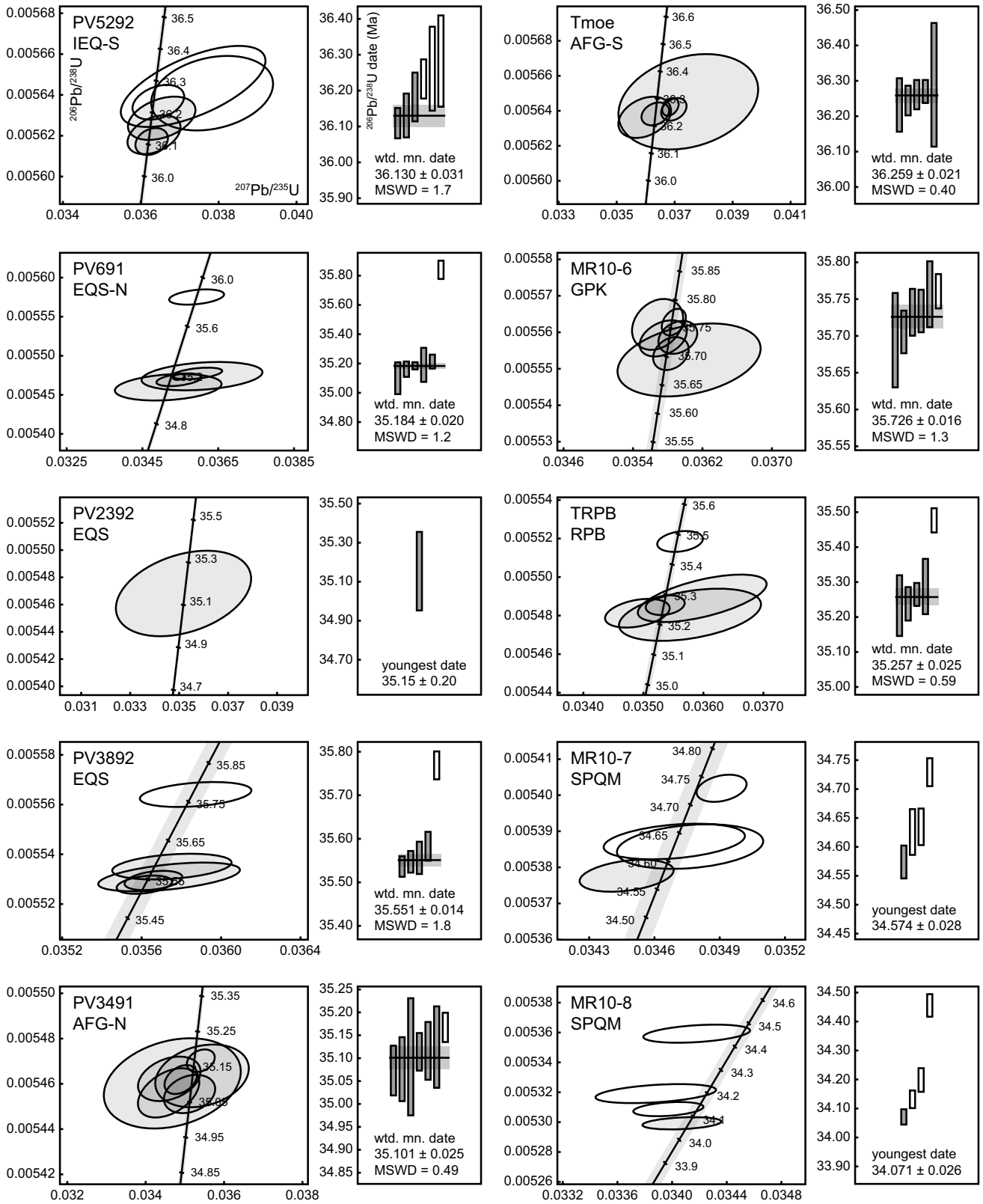

Fig. 2 continued

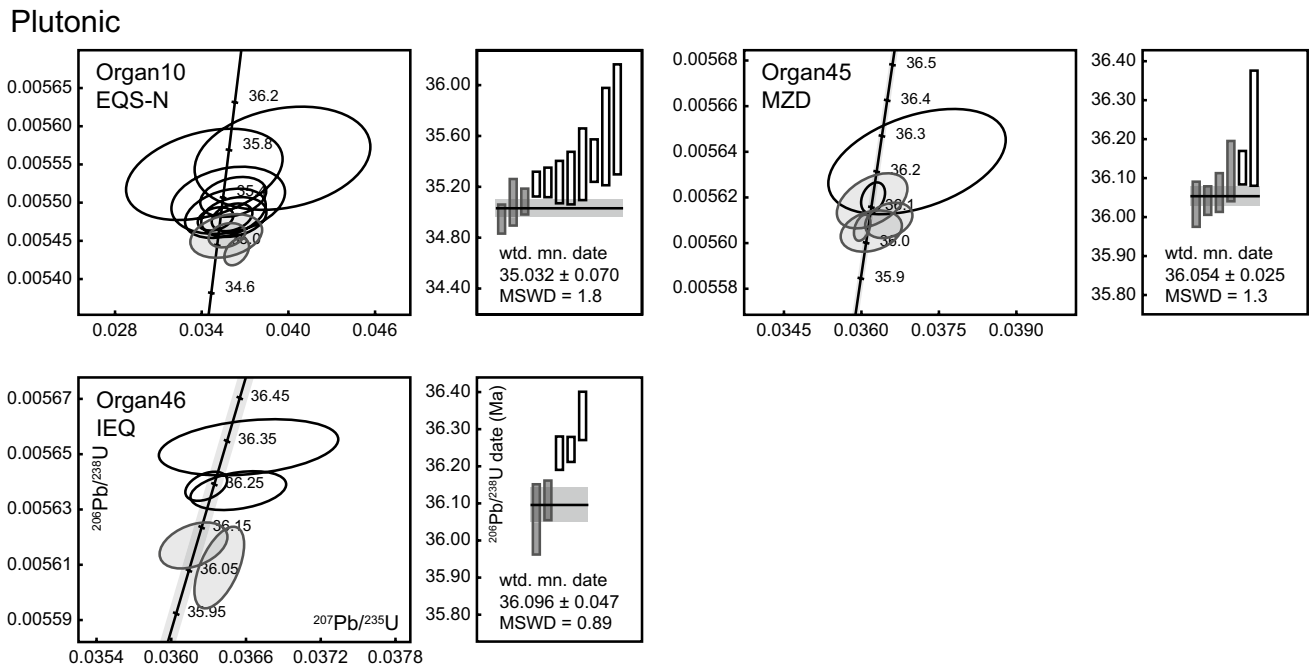

Fig. 3 Wetherill U-Pb concordia diagrams and weighted mean $^{206}Pb/^{238}U$ plots for samples dated at the University of North Carolina. Each data point is an analysis of a single-grain or small multi-grain fraction (n = 1–3 zircons). Axis labels are shown in the *lower left plot*. Two fractions from Organ10 with $^{206}Pb/^{238}U$ dates of ~ 80–90 Ma are excluded from the plot. Plot details and abbreviations follow Fig. 2

We interpret both fractions to be inherited xenocrystic zircons. The two samples of equigranular syenite from within the southern lobe yielded a weighted mean $^{206}Pb/^{238}U$ date of 35.551 ± 0.014 Ma (PV3892, MSWD = 1.8, n = 4/5) and a low-precision single zircon $^{206}Pb/^{238}U$ date of 35.15 ± 0.20 Ma (PV2392). The dates from these four samples are ~500–1000 ka younger than the seven other samples from the southern Organ Needle syenite.

Organ Needle monzodiorite

The Organ Needle monzodiorite has been interpreted as the most primitive phase of the Organ Needle pluton (Seager and McCurry 1988). A single sample from the monzodiorite yielded an interpreted weighted mean $^{206}Pb/^{238}U$ date of 36.054 ± 0.025 Ma (Organ45, MSWD = 1.3, n = 4/6). The date is within uncertainty of the youngest date from the Organ Needle syenites. In detail, the monzodiorite dates plot toward the younger end of the syenite dates; however, we are cautious about over-interpreting the relative dates for the two units because the monzodiorite is one of the three samples dated at UNC and we cannot discount the possibility of a small inter-laboratory bias. Based on this concern, we use the youngest syenite date (36.071 ± 0.012 Ma) as the final crystallization age of the Organ Needle pluton when calculating timescales of crystallization throughout.

Alkali feldspar granite

The three cupolas of AFG that intrude into the base of the Orejon Andesite and Cueva Tuff have been interpreted as the highest level exposures of the Organ Needle pluton (Fig. 1) (Seager and McCurry 1988; Vazquez and Lidzbarski 2012; Verplanck et al. 1995). Zircons from a sample from the middle exposure of the AFG yielded a single population of $^{206}Pb/^{238}U$ dates with a weighted mean of 36.259 ± 0.021 Ma (sample Tmoe, MSWD = 0.4, n = 5/5). This date is similar to, but slightly older than, the dates from the main syenite phase of the Organ Needle pluton. We did not date any samples from the southern AFG exposure; however, $^{40}Ar/^{39}Ar$ biotite cooling dates reported by Zimmerer and McIntosh (2013) suggest that the middle and southern AFG exposures are the same age; cooling dates from the middle and southern exposures are 36.25 ± 0.12 and 36.17 ± 0.12 Ma, respectively.

Zircons from the northern exposure of the AFG yielded a younger interpreted weighted mean $^{206}Pb/^{238}U$ of 35.101 ± 0.025 Ma (PV3491, MSWD = 0.49, n = 6/7). The younger date for the northern AFG (PV3491) overlaps the range of dates from the two northern syenite samples (PV691 and Organ10) and is significantly younger than the main southern phase of the Organ Needle pluton.

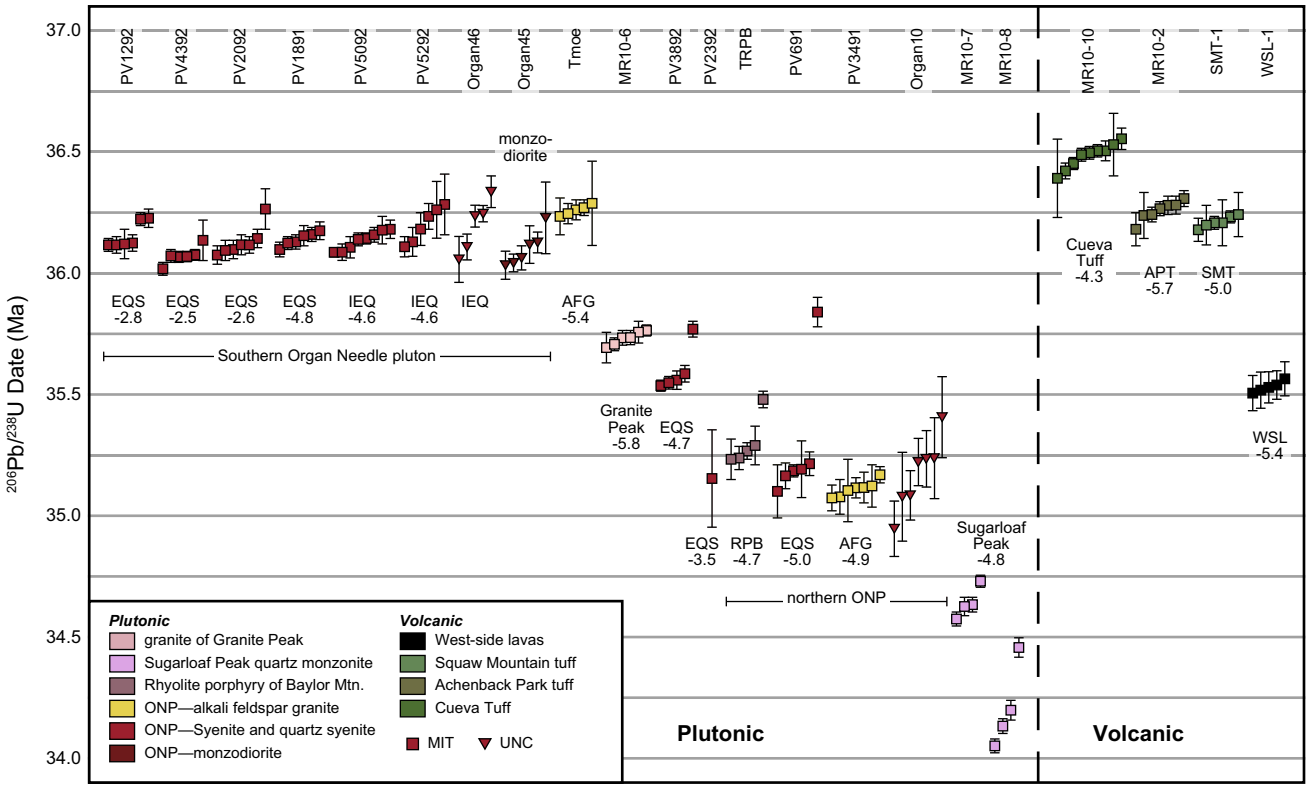

Fig. 4 Summary of the Th-corrected $^{206}Pb/^{238}U$ dates from the Organ Mountains. Symbol colors correspond to the map units in Fig. 1. Numbers are $\varepsilon_{Nd}(t)$ values from this study, Verplanck et al. (1995, 1999) and Butcher (1990); values for the Squaw Mountain tuff and West-side lavas are average values from other samples from these units, and Tmoe value is an average value for samples from the central and southern AFGs. For clarity, we excluded analyses with Th-corrected $^{206}Pb/^{238}U$ uncertainties greater than ±0.2 Ma and two fractions containing xenocrystic zircons from sample Organ10; the low-precision analyses are within uncertainty of the plotted higher precision dates. Abbreviations follow Fig. 2

Younger intrusive units

Zircons from the granite of Granite Peak and the rhyolite porphyry of Baylor Mountain yielded weighted mean $^{206}Pb/^{238}U$ dates of 35.726 ± 0.016 Ma (MR10-6, MSWD = 1.3, n = 5/6) and 35.257 ± 0.025 (TRPB, MSWD = 0.59, n = 4/4), respectively. Two samples from the Sugarloaf Peak quartz monzonite yielded variable $^{206Pb}/^{238U}$ dates. Zircons from MR10-7 and MR10-8 yielded $^{206}Pb/^{238}U$ dates from 34.729 ± 0.024 to 34.574 ± 0.028 Ma (n = 4) and 34.456 ± 0.039 to 34.051 ± 0.029 Ma (n= 4), respectively. The range of dates in each sample is most likely caused by significant inheritance of older zircons. We take the youngest date from the two samples (34.051 ± 0.029 Ma) as a maximum crystallization age for the Sugarloaf Peak quartz monzonite.

Sm–Nd and Rb–Sr isotopic data

Most of the dated samples were previously analyzed for major element and trace element geochemistry and Sm–Nd and Rb–Sr isotopic compositions by Verplanck et al. (1995, 1999). For the subset of new samples collected in this study, we report whole-rock Sm–Nd and Rb–Sr isotopic data (Table 2, Fig. 5). Seven samples from the Cueva Tuff, Achenback Park tuff, Squaw Mountain tuff, West-side lavas, granite of Granite Peak, Sugarloaf Peak quartz monzonite and rhyolite porphyry of Baylor Mountain have $\varepsilon_{Nd}(t)$ from −4.3 to −5.8 and $^{87}Sr/^{86}Sr(t)$ from 0.70561 to 0.72687.

Discussion

Progression of magmatism in the Organ Mountains caldera and batholith

The dated rocks record ~10 Ma of magmatism in the Organ Mountains from 44 to 34 Ma (Figs. 2, 3, and 4). The progression of magmatism is illustrated in Fig. 6 and outlined below.

Pre-Achenback Park tuff

A Paleozoic granite intruded by the Organ Mountains batholith recorded a U–Pb date of 1462 ± 28 Ma. The Orejon Andesite (44.215 ± 0.054 Ma) preserves the earliest

Table 1 Sample locations and descriptions

Sample	Latitude[a]	Longitude[a]	Map Unit[b]
Plutonic			
Organ10	32.3662	−106.5770	ONP equigranular syenite
Organ45	32.3284	−106.4874	ONP monzodiorite
Organ46	32.3501	−106.5277	ONP inequigranular syenite
MR10-6	32.3410	−106.5184	granite of Granite Peak
MR10-7	32.3671	−106.5594	SP quartz monzonite
MR10-8	32.4265	−106.5696	SP quartz monzonite
PV691[c]	32.4125	−106.5920	ONP equigranular syenite
PV1292[c]	32.2583	−106.5110	ONP equigranular syenite
PV1891[c]	32.3583	−106.5080	ONP equigranular syenite
PV2092[c]	32.2792	−106.5220	ONP equigranular syenite
PV2392[c]	32.2875	−106.5280	ONP equigranular syenite
PV3491[c]	32.4153	−106.5920	ONP alkali feldspar granite
PV3892[c]	32.2917	−106.5330	ONP equigranular syenite
PV4392[c]	32.3083	−106.4920	ONP equigranular syenite
PV5092[c]	32.3139	−106.4830	ONP inequigranular syenite
PV5292[c]	32.3153	−106.4830	ONP inequigranular syenite
Tmoe	32.3030	−106.5339	ONP alkali feldspar granite
TRPB	32.3927	−106.5848	Rhyolite porph. of Baylor Mtn.
Volcanic			
MR10-2	32.2993	−106.5833	Achenback Park tuff
MR10-10	32.2271	−106.5974	Cueva Tuff (Pena Blanca Tuff)
SMT-1	32.2936	−106.6074	Squaw Mountain tuff
WSL-1	32.3033	−106.6187	West-side lava
13-orejon-1	32.3371	−106.5931	Orejon Andesite
Wall rock			
06OR1	32.4103	−106.5907	Proterozoic granite

[a] WGS 84

[b] ONP, Organ Needle pluton; SP, Sugarloaf Peak

[c] Samples with geochemical and isotopic data reported in Verplanck et al. (1995, 1999). Locations for these samples were approximated from topographic maps

record of Cenozoic magmatism and predates the main phases of the Organ Mountains caldera by ~8 Ma, likely reflecting earlier subduction-related magmatism associated with the Laramide orogeny. The Cueva Tuff was subsequently erupted at 36.441 ± 0.020 Ma. There are no plutonic rocks as old as either the Orejon or Cueva eruptions in the Organ Mountains batholith, suggesting that either there was little or no plutonic record formed during these events or that any associated plutonic rocks are not exposed.

Achenback Park tuff, Squaw Mountain tuff and Organ Needle pluton

The largest volcanic and plutonic units were formed in rapid succession, but the new dates reveal small but important age differences. The two largest eruptive units, the Achenback Park and Squaw Mountain tuffs, were erupted at 36.259 ± 0.016 and 36.215 ± 0.016 Ma, respectively. The single-grain dates from the two units overlap within uncertainty, and the weighted mean dates are separated by 44 ± 23 ka, consistent with field observations suggesting minimal erosion between the two eruptions (Seager and McCurry 1988).

The differences in dates between these eruptive units and the underlying plutonic sequences are variable. $^{206}Pb/^{238}U$ dates from the central cupola of alkali feldspar granite overlap the data from the two tuffs within uncertainty, and the weighted mean date (36.259 ± 0.021 Ma) is the same as the eruption age for the Achenback Park tuff. The three units are also chemically and isotopically similar (Supplementary Figure SM4) (Butcher 1990; Seager and McCurry 1988; Verplanck et al. 1995, 1999), and the central and southern alkali feldspar granites likely represent the plutonic remnants of the magma chamber that fed one or both of these eruptions.

The zircon $^{206}Pb/^{238}U$ dates from the main southern portion of the Organ Needle pluton postdate the $^{206}Pb/^{238}U$ dates from the Achenback Park tuff, Squaw Mountain tuff and central AFG. Weighted mean $^{206}Pb/^{238}U$ dates from equigranular and inequigranular syenites range from 36.130 ± 0.031 to 36.071 ± 0.012 Ma, and the weighted mean date from the youngest sample is 144 ± 20 to 188 ± 20 ka younger than the weighted mean dates from the Squaw Mountain tuff and the central AFG/Achenback Park tuff, respectively. The dated syenite and quartz syenite samples come from throughout the southern extent of the Organ Needle pluton, include both equigranular and inequigranular portions of the pluton and have $\varepsilon_{Nd}(t) \approx -2$ to -5, suggesting that the main volume of the southern Organ Needle pluton intruded and/or underwent final crystallization over a short interval of 59 ± 33 ka. The dated sample from the Organ Needle monzodiorite (36.054 ± 0.025 Ma) is within uncertainty of the syenites. The relationship of the Organ Needle pluton to the tuff units is discussed in detail below.

Post-Organ Needle pluton

The mapped northernmost exposures of the syenitic phase of the Organ Needle pluton (hatched pattern in Fig. 1), the northern cupola of AFG, and the rhyolite porphyry of Baylor Mountain all significantly postdate intrusion of the main phase of the Organ Needle pluton. Samples from these units yielded weighted mean $^{206}Pb/^{238}U$ dates of 35.184 ± 0.020 Ma (syenite), 35.032 ± 0.070 Ma (syenite), 35.101 ± 0.025 Ma (AFG) and 35.257 ± 0.025 Ma (Baylor Mountain). The U–Pb dates suggest that these units crystallized in relatively rapid succession.

Table 2 Whole-rock Sm–Nd and Rb–Sr isotope data

Sample	Unit	Sm[a]	±2σ	Nd[a]	±2σ	$^{147}Sm/^{144}Nd$[b]	±2σ	$^{143}Nd/^{144}Nd$[b]	±2σ	$^{143}Nd/^{144}Nd_t$[c]	±2σ	$\varepsilon_{Nd}(t)$[c]	±2σ[d]
MR10-2	Achenback Park tuff	3.8471	0.0006	18.609	0.002	0.12507	0.00088	0.512328	0.000020	0.512298	0.000020	−5.72	0.45
MR10-3	Squaw Mountain tuff	7.4710	0.0060	29.810	0.008	0.15163	0.00107	0.512341	0.000014	0.512305	0.000014	−5.59	0.35
MR10-4	West-side lava	13.5150	0.0050	75.388	0.005	0.10846	0.00077	0.512383	0.000011	0.512358	0.000011	−4.57	0.30
MR10-6	Granite Peak	6.7220	0.0006	38.493	0.002	0.10565	0.00075	0.512318	0.000012	0.512293	0.000012	−5.83	0.32
MR10-8	Sugarloaf Peak	5.0695	0.0006	28.711	0.005	0.10682	0.00076	0.512370	0.000013	0.512346	0.000013	−4.84	0.33
MR10-10	Cueva Tuff	5.8930	0.0020	22.044	0.006	0.16173	0.00114	0.512409	0.000007	0.512370	0.000007	−4.30	0.25
TRPB	Baylor Mountain	4.2903	0.0006	23.997	0.002	0.10816	0.00076	0.512375	0.000012	0.512350	0.000012	−4.73	0.32
		Rb[a]	±2σ	Sr[a]	±2σ	$^{87}Rb/^{86}Sr$[b]	±2σ	$^{87}Sr/^{86}Sr$[b]	±2σ	$^{87}Sr/^{86}Sr_t$[c]	±2σ		
MR10-2	Achenback Park tuff	203.680	0.030	19.2177	0.0007	30.70	0.43	0.730747	0.000012	0.714972	0.000223		
MR10-3	Squaw Mountain tuff	302.046	0.007	7.1401	0.0003	123.04	1.73	0.774393	0.000014	0.711507	0.000889		
MR10-4	West-side lava	70.673	0.002	319.1600	0.0300	0.64	0.01	0.708482	0.000012	0.708158	0.000013		
MR10-6	Granite Peak	106.123	0.002	186.6800	0.0100	1.64	0.02	0.709683	0.000010	0.708849	0.000015		
MR10-8	Sugarloaf Peak	113.346	0.004	377.4100	0.0300	0.87	0.01	0.706025	0.000007	0.705605	0.000009		
MR10-10	Cueva Tuff	165.499	0.002	5.8629	0.0003	82.06	1.15	0.769098	0.000015	0.726873	0.000597		
TRPB	Baylor Mountain	224.213	0.006	32.9440	0.0020	19.69	0.28	0.717752	0.000013	0.707902	0.000140		

[a] Sm, Nd, Rb and Sr concentrations (ppm) determined by isotope dilution. All reported uncertainties are ±2σ absolute

[b] Fractionation, blank and spike-corrected isotopic ratios

[c] Initial ratios and ε_{Nd} calculated using preferred crystallization ages for the units as discussed in the text, present-day bulk Earth values of $^{143}Nd/^{144}Nd = 0.512638$ and $^{147}Sm/^{144}Nd = 0.1967$, $\lambda\ ^{147}Sm = 6.54 \times 10^{-12}$ year^{-1} (Lugmair and Marti 1978), and $\lambda^{87}Rb = 1.42 \times 10^{-11}$ year^{-1} (Davis et al. 1977)

[d] Uncertainties estimated following Ickert (2013)

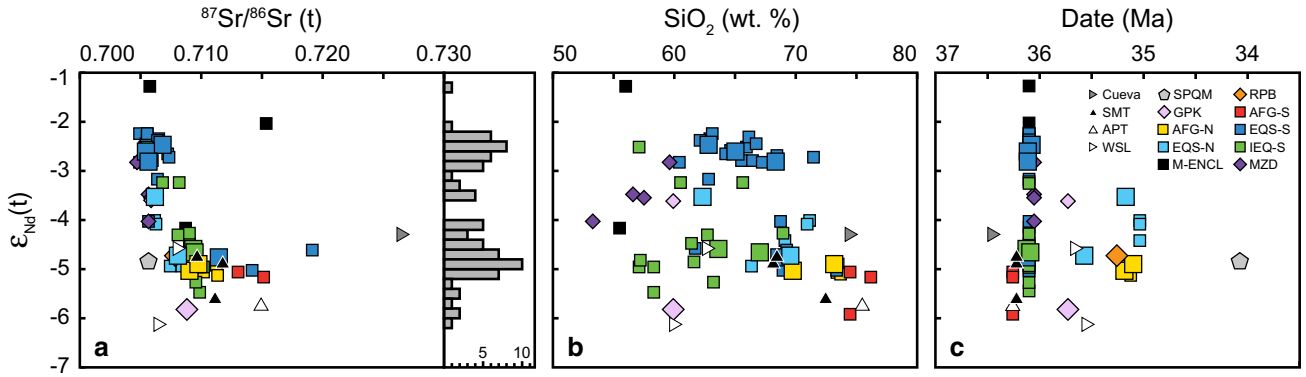

Fig. 5 Whole-rock Sm–Nd and Rb–Sr isotopic data from this study, Verplanck et al. (1995, 1999), Verplanck (1996) and Butcher (1990). **a** Initial $^{87}Sr/^{86}Sr$ versus $\varepsilon_{Nd}(t)$. Large symbols are dated samples. Smaller symbols are undated samples with ages inferred based on field relationships to dated samples. The right axis shows a histogram of $\varepsilon_{Nd}(t)$ for all of the existing plutonic and volcanic data. **b**. SiO_2 (wt%) versus $\varepsilon_{Nd}(t)$. **c**. Date (Ma) versus $\varepsilon_{Nd}(t)$. For undated Organ Needle syenite samples, we assumed a date of 36.098 Ma, calculated as the average of the dated syenite samples. Two analyses of a single sample of Squaw Mountain tuff (TssA6) from Butcher (1990) were excluded because repeat analyses yielded different $^{87}Sr/^{86}Sr$ and $\varepsilon_{Nd}(t)$. The two younger syenitic intrusions into the southern Organ Needle syenites (PV 2392 and PV3892) are plotted with the younger northern Organ Needle syenites. Abbreviations follow Fig. 2; M-ENCL, mafic enclaves within the southern syenites

Single-grain dates from the two syenites and one AFG sample overlap within uncertainty and permit the interpretation that these two units were co-magmatic. The Baylor Mountain porphyry appears to be slightly older; weighted mean dates indicate an interval of 156 ± 35 ka between the Baylor Mountain porphyry and the northern AFG. The age of these units is ~800–1000 ka younger than the main southern phase of the Organ Needle pluton, indicating that the northern arm of the Organ Needle pluton formed during a separate magmatic event. This observation is important because Verplanck et al. (1999) used geochemical trends between the main phase of the Organ Needle pluton and the northern quartz syenite and AFG to infer petrogenetic processes. The new dates require that the conclusions drawn from the geochemical trends be reassessed.

The older, southern portion of the Organ Needle pluton was also intruded by younger magmas. Two samples from exposures mapped as Organ Needle syenite yielded a weighted mean $^{206}Pb/^{238}U$ date of 35.551 ± 0.014 Ma (PV3892) and a single zircon $^{206}Pb/^{238}U$ date of 35.15 ± 0.20 Ma (PV2392). The dates are ~500–1000 ka younger than the surrounding Organ Needle syenites, and the younger sample is coeval with crystallization of the northern AFG and syenite. The older of the two samples has $\varepsilon_{Nd}(t) = -4.7$, whereas the adjacent syenites have $\varepsilon_{Nd}(t) \approx -2$. Verplanck et al. (1999) suggested this sample could reflect back mixing of marginal $\varepsilon_{Nd}(t) \approx -5$ magmas into the core of the Organ Needle pluton; the U–Pb dates suggest instead that the rock formed by intrusion of younger magma.

The granite of Granite Peak yielded a weighted mean $^{206}Pb/^{238}U$ date of 35.726 ± 0.016 Ma, indicating the parental magma intruded and crystallized between formation of the southern Organ Needle pluton and the later intrusions of the northern syenites and AFG. The West-side lavas erupted at 35.532 ± 0.030 Ma, within uncertainty of the crystallization age of the granite of Granite Peak. The Sugarloaf Peak quartz monzonite is the youngest intrusive unit, with a maximum crystallization age of 34.051 ± 0.029 Ma (MR10-8).

The volcanic–plutonic link

A key goal of this and previous work in the Organ Mountains has been to understand the link between epizonal plutonism and co-spatial volcanism. Seager and McCurry (1988) argued that smooth geochemical trends between the Cueva Tuff, Achenback Park tuff, Squaw Mountain tuff, and West-side lavas reflect progressive eruptions from a chemically zoned magma chamber, and suggested that the Organ Needle pluton may be the intrusive remnants of that chamber. Verplanck et al. (1999) similarly argued that the Organ Needle pluton is chemically stratified and that the AFG cupolas formed by differentiation of the $\varepsilon_{Nd}(t) \approx -5$ inequigranular syenites exposed at the base of the Organ Needle pluton. They suggested that the AFG cupolas erupted to form the Squaw Mountain tuff. Zimmerer and McIntosh (2013) presented $^{40}Ar/^{39}Ar$ dates from the Cueva Tuff (36.45 ± 0.08 Ma), Achenback Park tuff (36.23 ± 0.14 Ma) and Squaw Mountain tuff (36.03 ± 0.16 Ma; 2σ internal), which all overlap within uncertainty, and concluded

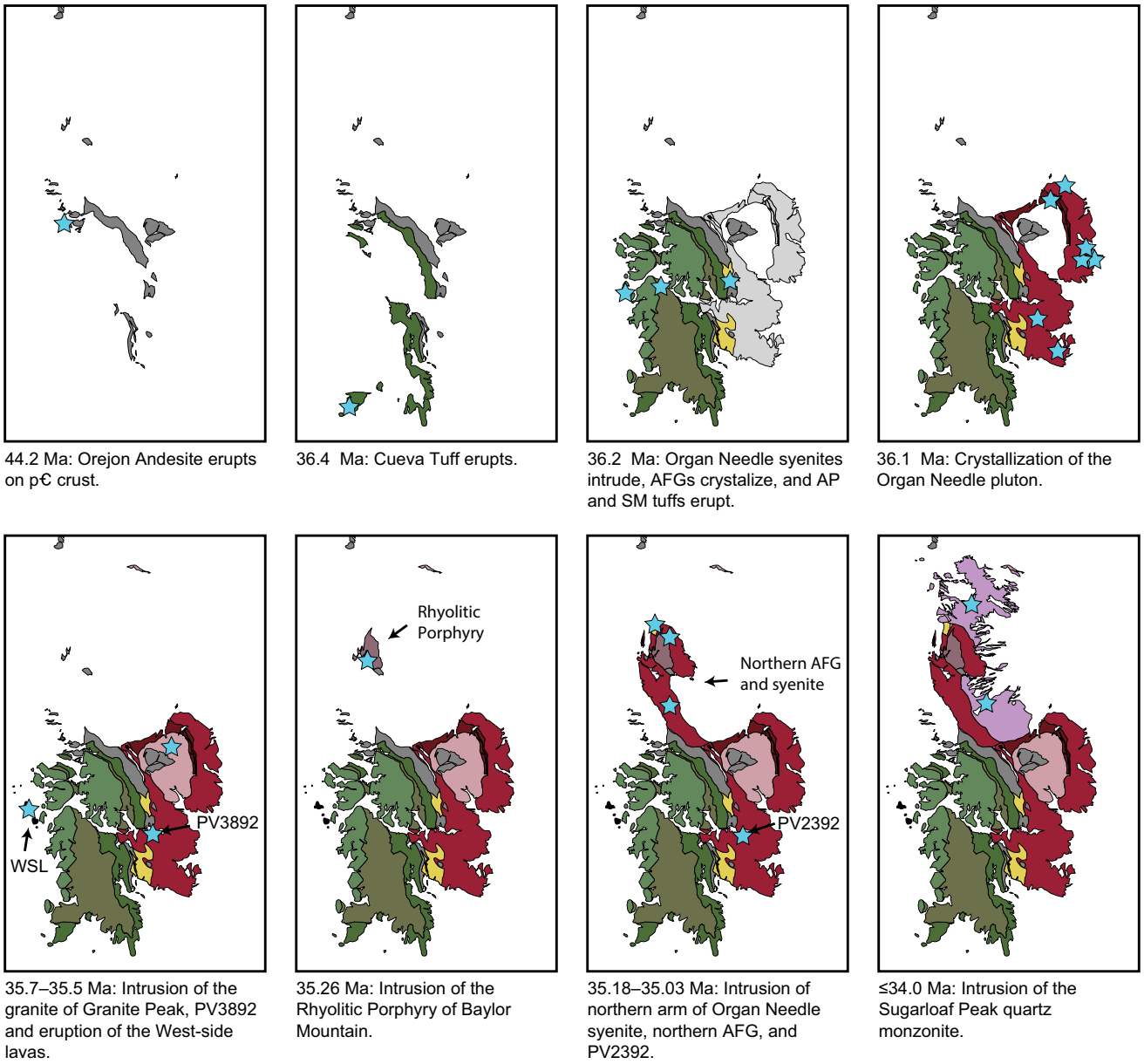

Fig. 6 Progression of plutonism and volcanism in the Organ Mountains caldera and batholith, based on the U-Pb dates from this study. Blue stars mark the location of dated samples in each time step. Map location and key are the same as Fig. 1. *AP* Achenback Park, *SM* Squaw Mountain

that all of the tuffs may have erupted from a long-lived (420 ± 240 ka) magma chamber in the upper crust.

The new U–Pb dates provide a more precise record of the volcanic history and directly date the timing of pluton crystallization, allowing for a more detailed comparison. The small offset in crystallization ages between the main phase of the Organ Needle pluton, and the Achenback Park tuff (188 ± 20 ka), Squaw Mountain tuff (144 ± 20 ka) and central AFG (188 ± 24 ka) could reflect a range of different processes. Three potential explanations are as follows: (1) The volcanic units and AFG formed from an older magma, which crystallized prior to intrusion of the syenitic phase of the Organ Needle pluton; (2) all of the units are genetically related and reflect evolution of the magmatic system over tens to hundreds of thousands of years; or (3) all of the units are synchronous, but the older dates for the Achenback Park tuff, Squaw Mountains tuff and AFG reflect magma residence for the zircons prior to eruption. We discount the latter model, because it is unlikely that the tuff eruptions would not include younger zircons recorded in the plutonic record, there is good agreement between the tuff dates and the plutonic AFG, and the tuff dates overlap

within uncertainty with reported $^{40}Ar/^{39}Ar$ dates (Zimmerer and McIntosh 2013).

It is not possible to definitively differentiate between the first two hypotheses. In the field, the AFGs appear to grade into the more massive syenitic phase of the Organ Needle pluton over distances of centimeters to meters (Seager and McCurry 1988). Geochemical data from the middle and southern AFG cupolas plot along fractionation trends with the Organ Needle syenites, for both major elements and trace element ratios such as Th/U and La/Yb (Supplementary Figure SM3) (Verplanck et al. 1995, 1999). These trends support the Verplanck et al. (1995, 1999) interpretation that the AFG formed by differentiation of the $\varepsilon_{Nd}(t) \approx -5$ syenitic magmas at the base of the Organ Needle pluton. Verplanck et al. (1999) further argued that low concentrations of P_2O_5, Sr, and the light rare earth elements (LREE), low normalized La/Yb, and negative Eu anomalies in the AFG (Supplementary Figure SM3) are consistent with plagioclase, apatite and titanite fractionation. Chemical and textural evidence suggests that the inequigranular syenites from the base of the Organ Needle pluton contain these cumulate phases and could represent the residual solids from differentiated AFG magmas, suggesting a genetic link between the syenites and the AFG. These chemical relationships are apparent even when considering just the central and southern AFG, and excluding the younger northern AFG. Finally, the middle and southern AFGs also have $\varepsilon_{Nd}(t) = -5.9$ to -5.1, which overlap, but extend to slightly lower values than, the low $\varepsilon_{Nd}(t)$ portions of the Organ Needle syenites (-3.2 to -5.5). Taken together, these observations permit a genetic relationship between the main syenitic phase of the Organ Needle pluton and the middle and southern AFGs, but do not require such a relationship, as demonstrated by the similar chemical trends in the northern syenite and AFG, which significantly postdate the main southern phase of Organ Needle plutonism.

The U–Pb zircon systematics in the Organ Needle syenites may reflect a protracted magmatic history. Although the youngest dated zircons in the southern Organ Needle syenites are systematically younger than zircons from the AFG, Achenback Park tuff and Squaw Mountain tuff, six of the seven samples recorded a range of dates larger than analytical uncertainties, and the oldest dates in these samples overlap within uncertainty with the youngest dates in the AFG, Achenback Park tuff and Squaw Mountain tuff (Fig. 4).

Given the geochemical trends, similar isotopic compositions, and the duration of U–Pb dates in the Organ Needle syenites, we favor the interpretation that the Achenback Park tuff, Squaw Mountain tuff, middle and southern AFGs, and Organ Needle syenites are genetically related and formed from a long-lived magmatic system. This interpretation implies that some form of magma chamber or mush zone persisted just below the volcanic system for a period of $\geq 188 \pm 20$ ka—calculated as the difference between the eruption age of the Achenback tuff (MR10-2) and the youngest crystallization age for the Organ Needle pluton syenites (PV4392)—although the system may have been at near-solidus conditions for large portions of this time period (Cooper and Kent 2014). The similar isotopic composition and the complementary trace element trends described above suggest that the alkali feldspar granite, Achenback Park tuff and Squaw Mountain tuff may represent felsic differentiates from the $\varepsilon_{Nd}(t) \approx -5$ inequigranular syenites. A detailed model for the development of the system is presented below.

Some of the observed offset between the Organ Needle pluton and the central AFG and Squaw Mountain tuff may reflect variable zircon saturation temperatures in the crystallizing magmas. Zircon saturation temperatures were calculated using the Watson and Harrison (1983) zircon solubility model and existing whole-rock geochemical data from the Organ Mountains system (Butcher 1990; Verplanck 1996; Verplanck et al. 1995, 1999). Although the whole-rock data from plutonic samples likely do not reflect melt compositions, calculated zircon saturation temperatures are insensitive to compositional variations as a result of addition of cumulate feldspar (<2 °C variations for addition of up to 20 % cumulate feldspar). The Organ Needle syenites, Achenback Park tuff, southern AFG and Squaw Mountain tuff have average zircon saturation temperatures of 821, 826, 858 and 882 °C, respectively (Table 3). The range of saturation temperatures suggests that even if all of the parental magmas formed synchronously, the southern AFG and the parental magma to the Squaw Mountain tuff would have started to crystallize zircon 35 to 60 °C earlier than the Organ Needle syenites (assuming zircon saturated in the magma prior to eruption of the Squaw Mountain tuff), potentially explaining some of the offset in ages between these units. However, the Achenback Park tuff has similar zircon saturation temperatures to the Organ Needle syenites, suggesting the older dates from this unit and the offset dates between the volcanic units and the Organ Needle syenites are not just related to a higher zircon liquidus temperatures.

Table 3 Zircon saturation temperatures

Unit	Min.[a] (°C)	Max.[a] (°C)	Ave.[a] (°C)	n[b]
Organ Needle syenites	731	891	821	38
Achenback Park tuff	795	841	826	6
Squaw Mountain tuff	841	925	882	23
Southern AFG	796	880	858	6

[a] Minimum, maximum and average zircon saturation temperatures (Watson and Harrison 1983) calculated using whole-rock geochemical data of Verplanck et al. (1995, 1999), Verplanck (1996) and Butcher (1990)

[b] Number of data points

The northern Organ Needle syenites and associated AFG cupola have similar compositions and geochemical trends to the southern syenites and AFG (Supplementary Figure SM3), despite being ~1 Ma younger. The temporal evolution of the northern syenites and AFG is not as precisely constrained; however, it seems likely that the northern and southern bodies formed by similar magmatic processes that episodically generated syenitic parental magmas, which differentiated to form alkali feldspar granite caps, which then erupted as silicic tuffs (any volcanic record is not preserved for the younger northern syenite-AFG system).

The U–Pb dates from the West-side lavas and granite of Granite Peak overlap within uncertainty, suggesting that the West-side lavas may represent the extrusive equivalent of the granite of Granite Peak.

Magma fluxes and plutonic cooling rates

The precise U–Pb dates can be used to estimate the magmatic fluxes during formation of the Organ Needle pluton (see the Supplementary Text for details on the flux calculations). The calculated magmatic fluxes depend on what units are included as part of the pluton. In our preferred model, the southern and central AFGs and the main southern body of Organ Needle pluton syenites all formed from a single long-lived magma chamber/mush zone. The total lifespan of the magma chamber/mush zone is then 188 ± 24 ka, requiring minimum magmatic fluxes of 0.0006–0.0008 km^3/year. If instead the AFG formed from an earlier unrelated magma, the duration of Organ Needle pluton magmatism was 59 ± 33 ka, requiring higher magma fluxes of 0.002–0.003 km^3/year. These rates are similar to calculated fluxes of other well-studied plutons from magmatic arcs and silicic caldera systems (0.0001–0.003 km^3/year) (e.g., Davis et al. 2012; Matzel et al. 2006; Mills and Coleman 2013; Tappa et al. 2011). If the Achenback Park tuff and Squaw Mountain tuff are included in the flux, the minimum total plutonic plus volcanic magmatic flux is 0.002 km^3/year. If the pluton is thicker than the exposed section or mafic cumulates are preserved at depth, the magmatic fluxes could be significantly higher.

Recent numerical thermal models have studied the timescales of crystallization in periodically recharged shallow crustal magma chambers. The duration of crystallization is dependent of the magmatic flux. Numerical modeling by Annen (2009) suggests that at magmatic fluxes of 0.003–0.005 km^3/Ma, similar to the minimum combined magmatic and volcanic flux of ≥0.002 km^3/year calculated above, a mush zone (>40 % melt) can be established in ~30–100 ka (incubation period) and reach a maximum volume of ~20–30 % of a cylindrical silicic pluton with a diameter and depth of 10 km, emplaced at a depth of 5 km in the crust. The exposed area of the Organ Needle pluton has a diameter of ~12 km, but the total depth of the pluton is poorly constrained.

Gelman et al. (2013) carried out similar numerical models using a nonlinear crystallization–temperature relationship and temperature-dependent thermal conductivity, which resulted in higher melt volumes at a given magmatic flux. For fluxes of 0.00314–0.00525 km^3/Ma, the mean melt fractions ranged from ~8 to 55 % and the modeled plutons crystallized over periods of <0.02–0.7 Ma; modeled plutons had a 20 km diameter and 10 km depth and were emplaced at 5 km depth in the crust. The numerical thermal models therefore permit the interpretation that the southern AFG, Squaw Mountain tuff, Achenback tuff and Organ Needle syenites formed from a long-lived magmatic system that was active for ≥188 ± 20 ka.

The proposed lifespan of the magmatic system is also consistent with magma residence times of 10^4–10^5 years based on U-series, U–Pb and $^{40}Ar/^{39}Ar$ dating of accessory and major minerals in volcanic samples (Brown and Fletcher 1999; Cooper and Kent 2014; Cooper and Reid 2008; Reid 2014; Reid et al. 1997; Schoene et al. 2012; Simon et al. 2008; Vazquez and Reid 2002).

Isotopic constraints on magma evolution in the Organ Mountains

The majority of the Sm–Nd isotopic data from the Organ Mountains system form two clusters at $\varepsilon_{Nd}(t) \approx -2.5$ and −5; out of the 76 whole-rock analyses from volcanic and plutonic rocks from the Organ Mountains system, 25 cluster between $\varepsilon_{Nd}(t)$ of −2.2 and −2.8 and 39 fall between $\varepsilon_{Nd}(t)$ of −4.0 and −5.5 (Fig. 5) (this study; Butcher 1990; Verplanck 1996; Verplanck et al. 1995, 1999). A small group of five samples have $\varepsilon_{Nd}(t) < -5.5$ (Fig. 5); however, all but one of these samples are from units that record a range of isotopic compositions. Multiple analyses from different samples of the Squaw Mountain tuff, West-side lavas, central-southern AFG and granite of Granite Peak have $\varepsilon_{Nd}(t)$ of −4.7 to −5.8 ($n = 4$), −4.6 to −6.1 ($n = 2$), −5.1 to −5.9 ($n = 3$) and −3.6 to −5.8 ($n = 2$), respectively. A single sample from the Achenback tuff has an $\varepsilon_{Nd}(t) = -5.7$. The variable values for these units could reflect true heterogeneity in the isotopic composition of the magmas or analytical scatter. For the volcanic rocks, the low $\varepsilon_{Nd}(t)$ data may also reflect incorporation of xenocrysts or lithic fragments from Proterozoic wall rocks [$\varepsilon_{Nd}(t) < -10$] in some of the analyzed samples.

The combined whole-rock isotopic data and U–Pb dates indicate that the $\varepsilon_{Nd}(t) \approx -5$ magmas were intruded and erupted in the Organ Mountains system over a period of ≥2.4 Ma, from eruption of the Cueva Tuff to intrusion of the Sugarloaf Peak quartz monzonite (Fig. 5c). This observation suggests that either (1) partial melting and

assimilation of wall rocks into a parental magmas with higher $\varepsilon_{Nd}(t)$ resulted in magmas with a consistent isotopic composition over long time periods, or (2) the magmas were derived from a homogenous source with $\varepsilon_{Nd}(t) \approx -5$.

Verplanck et al. (1995, 1999) showed that mafic enclaves within both the equigranular [$\varepsilon_{Nd}(t) \approx -2.5$] and inequigranular [$\varepsilon_{Nd}(t) \approx -5$] Organ Needle syenites have $\varepsilon_{Nd}(t) = -1.3$ to -2, likely reflecting a parental magma composition with similar or higher $\varepsilon_{Nd}(t)$. They further showed that partially melted xenoliths of the Proterozoic wall rock occur within the inequigranular syenite and that the $\varepsilon_{Nd}(t) \approx -5$ magmas could have been generated by mixing of a parental magma composition similar to the mafic enclaves and partial melts of the Proterozoic wall rocks at shallow crustal levels. These data demonstrate that wall rock assimilation was at least locally important and that the $\varepsilon_{Nd}(t) \approx -5$ magmas in the Organ Needle pluton could be related to melting and assimilation of Paleozoic to Proterozoic wall rocks into parental magmas with higher $\varepsilon_{Nd}(t)$ at shallow crustal levels.

If the consistent $\varepsilon_{Nd}(t) \approx -5$ magmatism over 2.4 Ma in the Organ Mountains system was generated by a similar process, it could suggest some fundamental control on the degree of wall rock melting or the composition of the partial melts. Given that the analyzed wall rocks have $\varepsilon_{Nd}(t) < -10$, there is no a priori reason that wall rock assimilation would consistently lead to $\varepsilon_{Nd}(t) \approx -5$ magmas, rather than a range of compositions. One possibility is that partial melts from the wall rocks have a different composition than the analyzed whole rocks; variable Sm/Nd in different minerals in the wall rocks could lead to variable $^{143}Nd/^{144}Nd$, which could in turn result in a liquid with a different isotopic composition than the whole rock during partial melting. However, isotopic data from Verplanck et al. (1999) indicate that this explanation is unlikely because $\varepsilon_{Nd}(t)$ from analyzed samples of both the Proterozoic wall rocks and partially melted xenoliths are similar.

Alternately, the consistent $\varepsilon_{Nd}(t)$ could reflect a relatively constant ratio for the volume of parental magma to the volume of assimilated partial melt, assuming both had constant compositions. This model would suggest that the integrated volume of intruded magma was the same order of magnitude in each of the major phases of magmatism during formation of the batholith and caldera; however, such a process would be fortuitous.

We consider it more likely that silicic $\varepsilon_{Nd}(t) \approx -5$ magmas in the Organ Needle system were generated by partial melting of the lower crust, rather than melting and assimilation of the Proterozoic wall rocks. Jacob et al. (2015) used whole-rock geochemistry and isotopic data to argue that small-volume silicic epizonal plutons, and associated volcanic rocks, in the Never Summer igneous complex, north-central Colorado, were generated by such a process. In the Never Summer system, evidence from crustal xenoliths entrained in Devonian kimberlites shows that Precambrian mafic lower continental crust beneath this portion of the southern Rocky Mountains has Nd and Sr isotopic compositions identical to those observed for silicic intrusive rocks and related, small-volume topaz rhyolites. The Organ Mountains system shares a similar geologic setting to the Never Summer igneous complex, as both are small-volume igneous centers that formed at the periphery of large-volume igneous centers (the Mogollon-Datil and southwestern Colorado volcanic fields, respectively). The two systems also formed within a thick section of Paleoproterozoic continental lithosphere: the Mazatzal province in New Mexico and the Yavapai province in Colorado. The isotopic compositions of the Never Summer and Organ Mountains system are also similar. High-silica intrusive rocks in the Never Summer system have $\varepsilon_{Nd}(t) \approx -5$ to -6, and the most radiogenic rocks have $\varepsilon_{Nd}(t) \approx 0$ to -2.

The consistent $\varepsilon_{Nd}(t) \approx -5$ magmatism within the Organ Mountains system may therefore reflect partial melting of $\varepsilon_{Nd}(t) \approx -5$ lower crust by mantle-derived basaltic magmas with $\varepsilon_{Nd}(t) = -1.3$ to -2, as constrained by the isotopic composition of mafic enclaves. More robust testing of this hypothesis is limited by the lack of available lower crustal xenoliths in pre-Cenozoic volcanic rocks from New Mexico, which could constrain the chemical and isotopic compositions of the lower continental crust during Organ Mountains magmatism.

The evolved composition of the Organ Mountains system is consistent with formation by epizonal differentiation of silicic lower crustal partial melts. The exposed southern Organ Needle syenites, Organ Needle monzodiorite, and the middle and southern AFGs have basaltic trachyandesite to rhyolitic compositions with an approximate average of ~64 wt% SiO_2—estimated by weighting the average of published chemical data by the exposed area for each unit. The preserved plutonic section is too felsic to represent closed-system fractionation of basaltic magma, suggesting that either a silicic parental magma was delivered to shallow crustal magma chambers from deeper in the crust, or mafic residues from basaltic differentiation are preserved below the current levels of exposure.

Overall, a consistent interpretation of the available data is that $\varepsilon_{Nd}(t) \approx -2$ basaltic magmas intruded and partially melted an $\varepsilon_{Nd}(t) \approx -5$ lower crust. The $\varepsilon_{Nd}(t) \approx -5$ magmas then rose into the upper crust. The scatter in the isotopic data ($\varepsilon_{Nd}(t) = -4$ to -6), if they do reflect true isotopic heterogeneity of the magmas, may reflect heterogeneities within the lower crust. The isotopic zonation in the southern Organ Needle pluton may represent rejuvenation of an $\varepsilon_{Nd}(t) \approx -5$ mush zone by underplating of mafic $\varepsilon_{Nd}(t) \approx -2$ magmas. A lower crustal origin

for the $\varepsilon_{Nd}(t) \approx -5$ magmatism in the Organ Mountains is attractive because it allows for a low flux of silicic anatectic melts, with isotopic compositions fixed by the mafic crust undergoing melting, to be delivered to the upper crust through the entire ≥2.4 Ma period of active magmatism. Once the silicic melts arrived in the upper crust, they underwent further differentiation. Sills of silicic melts that at least partially solidified in the upper crust early in the magmatic system's history may have provided a ready source of silicic melt when reheated by underplated mafic magmas.

Temporal constraints on models of ignimbrite formation

Tappa et al. (2011) and Mills and Coleman (2013) have argued that the relative timing of plutonism and volcanism in silicic caldera systems can be used to differentiate between end-member models for rhyolite formation. Models for the generation of ignimbrites and shallow level plutonic systems can be broadly described as down-temperature magma crystallization models or up-temperature partial melting models (Bachmann and Bergantz 2008; Mills and Coleman 2013). In down-temperature models, rhyolitic magmas are formed by differentiation of mafic magmas in crustal chambers or mush zones (e.g., Bachmann and Bergantz 2004, 2008; Cooper and Kent 2014; Halliday et al. 1991; Lipman 1984). The silicic magmas can erupt to form ignimbrites, and the residual solids are preserved as plutonic rocks. In contrast, in the up-temperature models, silicic magmas are generated by partial melting of existing lower crustal rocks (e.g., Glazner et al. 2004; Mills and Coleman 2013; Tappa et al. 2011). It has been posited that the formation of plutonic versus volcanic deposits is then dependent on the magmatic flux; high magma fluxes favor the eruption of silicic magmas as large ignimbrites, whereas lower magma fluxes lead to crystallization of magmas as plutonic rocks in the upper crust and smaller scale volcanic eruptions (Glazner et al. 2004; Mills and Coleman 2013; Tappa et al. 2011). As a consequence, plutonic rocks may be emplaced during the waxing and waning stages of magmatic cycles.

Tappa et al. (2011) and Mills and Coleman (2013) studied coupled caldera and epizonal plutonic systems in the Latir volcanic field, New Mexico, and the Mount Princeton magmatic center, Colorado. In the Latir volcanic field, the dated plutonic rocks postdate eruption of the largest ignimbrite by 0.23 ± 0.08 to 2.93 ± 0.08 Ma, with all but one dated sample being ≥0.43 ± 0.07 Ma younger. In the central Colorado volcanic field, the Mount Princeton Quartz Monzonite crystallized during an apparent 1.9 ± 0.3 Ma gap in ignimbrite activity. The offsets in plutonic and volcanic activity in these areas were interpreted to favor up-temperature models, where the silicic magmas were formed by partial melting in the lower crust, and the offset between plutonic and volcanic activity resulted from changes in magma fluxes.

Our new data from the Organ Mountains system indicate that peak volcanism and plutonism were more closely temporally related. The largest volcanic and plutonic units are the Achenback Park tuff, the Squaw Mountain tuff, and the Organ Needle pluton, and U–Pb dates suggest the two tuffs erupted 0.188 ± 0.020 and 0.144 ± 0.020 Ma prior to final crystallization of the Organ Needle pluton. This age difference is small compared to the offsets observed in the Latir and Mount Princeton studies, and given the small offset in ages and similar geochemical trends between the Achenback Park tuff, Squaw Mountain tuff and Organ Needle pluton, our preferred interpretation is that the volcanic and plutonic rocks are genetically related and formed from a long-lived magma chamber/mush zone.

However, the data do not preclude up-temperature models for ignimbrite formation and are equivocal concerning the hypothesis that the formation of volcanic versus plutonic rocks is related to magmatic flux. As discussed above, we favor the interpretation that at least part of the Organ Mountains system formed from silicic lower crustal melts, based on the consistent $\varepsilon_{Nd}(t) \approx -5$ isotopic composition of the system through time, and similarities to the Never Summer magmatic system (Jacob et al. 2015). In terms of magmatic fluxes, the overall dataset from the Organ Mountains could be interpreted to reflect a progressive shift from large-scale volcanic eruptions prior to eruption of the Squaw Mountain tuff at 36.215 ± 0.016 Ma, to a dominantly plutonic system after this eruption (Fig. 4), perhaps reflecting a change in the magma fluxes. However, this is largely speculative, as large-scale volcanism associated with the Sugarloaf Peak plutonism and the younger syenites and AFG in the northern arm of the Organ Needle pluton may simply not be exposed above the West-side lavas.

The more compressed timeline in the Organ Mountains compared to the Latir and Mount Princeton systems (Mills and Coleman 2013; Tappa et al. 2011) may also be related to the size of the studied magmatic systems. Mills and Coleman (2013) compiled estimated magma fluxes for plutonic and volcanic rocks and argued that there may be fundamental differences between large-volume (>500 km^3) and small-volume (<500 km^3) volcanic eruptions, and that smaller eruptions may be associated with plutonism. The Latir and Mount Princeton systems both have estimated erupted volumes ≥500 km^3. In contrast, the total magma volume for the Organ Needle pluton, Achenback Park tuff, and Squaw Mountain tuff is ~360 km^3 (Supplementary Text), placing it in the lower flux regime. If the Mills and Coleman (2013) model is correct, the relative timing of plutonism and volcanism may not be a useful measure for

discriminating between up-temperature and down-temperature models in small to intermediate magmatic systems.

A revised petrogenetic model

The new U–Pb dates and isotopic data better constrain the formation and evolution of the Organ Mountains caldera and batholith. Here we present a revised petrogenetic model for the formation of the Organ Needle pluton, central and southern AFGs, Achenback Park tuff, and Squaw Mountain tuff that incorporates both our new data, and the extensive previous mapping and whole rock and mineral geochemistry from this area (Butcher 1990; Seager 1981; Seager and McCurry 1988; Verplanck 1996; Verplanck et al. 1995, 1999). We limit the model to these units because they are the best studied and our data suggest they may be co-genetic. The model builds on, and modifies, the four-step model presented in Verplanck et al. (1999). The model is illustrated schematically in Fig. 7; the preexisting volcanic (Cueva Tuff and Orejon Andesite) and plutonic units are not separately delineated for simplicity. The proposed model is consistent with all of the available data, but is not uniquely constrained, and should be tested by further field and analytical work.

1. Prior to 36.26 Ma, mantle-derived basaltic magmas with $\varepsilon_{Nd}(t) \approx -1$ to -2 intruded and partially melted the lower crust, generating silicic partial melts with $\varepsilon_{Nd}(t) \approx -5$. These silicic melts rose into an epizonal magma chamber within Proterozoic wall rocks, which have $\varepsilon_{Nd}(t) < -10$. The magmas likely underwent some differentiation during transport and within the shallow level chamber, potentially leading to some vertical chemical stratification.
2. At 36.26–36.22 Ma, the $\varepsilon_{Nd}(t) \approx -5$ crystal mush was underplated by a single pulse or multiple pulses of basaltic $\varepsilon_{Nd}(t) \approx -2$ magma. The recharge event rejuvenated the $\varepsilon_{Nd}(t) \approx -5$ mush zone. The structurally highest $\varepsilon_{Nd}(t) \approx -5$ AFG that forms the central and southern cupolas may have either formed prior to the recharge event, or more likely, may be a direct result of partial melting of the $\varepsilon_{Nd}(t) \approx -5$ mush zone during basaltic underplating. In either case, the basaltic underplating likely triggered eruption of the AFG magmas to form the Achenback Park and Squaw Mountain tuffs. Decompression and cooling at the top of the chamber during one or both of the eruptions led to the rapid solidification of the AFG, as reflected by their older U–Pb date (Fig. 4). Trace element data from the AFG and Organ Needle pluton are consistent with the inequigranular syenites from the base of the pluton representing residual solids removed from the AFG magmas.
3. Continued recharge and differentiation led the underplated $\varepsilon_{Nd}(t) \approx -2$ magma to rise into and displace

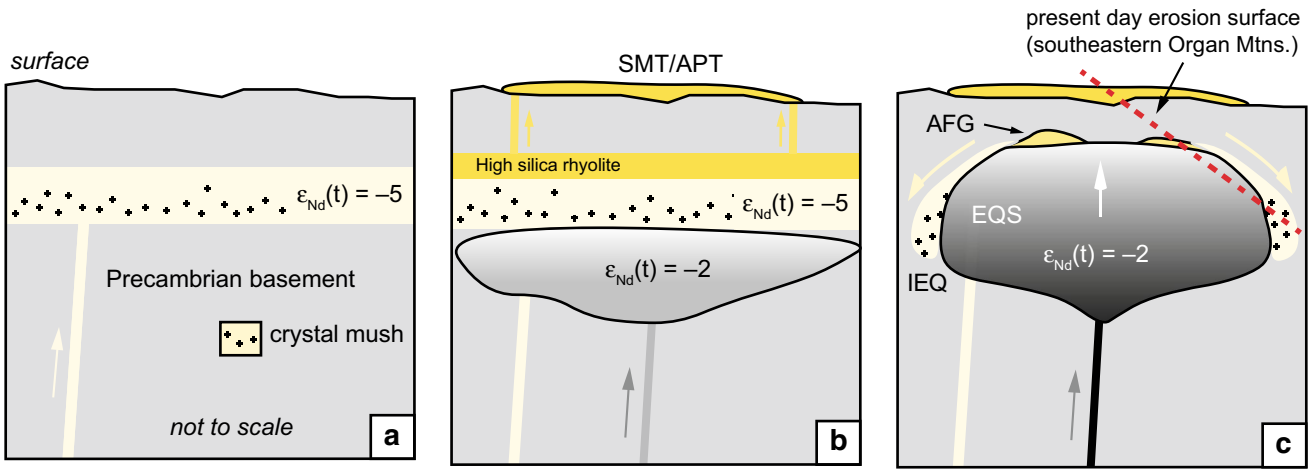

>36.26 Ma: Emplacement of early, silicic, $\varepsilon_{Nd}(t) = -5$, lower crustal melts

36.26–36.22 Ma: Underplating by $\varepsilon_{Nd}(t) = -2$ magma, generation of high silica rhyolite by partial melting of the $\varepsilon_{Nd}(t) = -5$ mush zone, and eruption of the APT and SMT

36.22–36.10 Ma: Continued underplating, rise of underplated magma, down welling of crystal mush, final crystallization of the inequigranular (IEQ) and equigranular (EQS) syenites

Fig. 7 Schematic petrogenetic model for the intrusion of the Organ Needle pluton, and southern alkali feldspar granites, and eruption of the Achenback Park tuff and Squaw Mountain tuff. *AFG* alkali feldspar granite, *IEQ* inequigranular syenite, *EQS* equigranular syenite, *APT* Achenback Park tuff, *SMT* Squaw Mountain tuff, *AFG* alkali feldspar granite

the overlying mush zone. The $\varepsilon_{Nd}(t) \approx -5$ magma was smeared out along the margins of the $\varepsilon_{Nd}(t) \approx -2$ core, accounting for the current isotopic zoning observed in the Organ Needle syenites. We note that although the $\varepsilon_{Nd}(t) \approx -5$ magmas occur along the margins of the $\varepsilon_{Nd}(t) \approx -2$ pluton, the absence of a correlation between 1/Nd and $\varepsilon_{Nd}(t)$ for the $\varepsilon_{Nd}(t) \approx -5$ rocks suggests that they formed by differentiation of a parental $\varepsilon_{Nd}(t) \approx -5$ magma, as implied in this petrogenetic model, rather that in situ assimilation of the Proterozoic wall rock into $\varepsilon_{Nd}(t) \approx -2$ magmas (Verplanck et al. 1995).

4. Following eruption of the Achenback Park and Squaw Mountain tuffs, the equigranular and inequigranular syenites cooled and crystallized over 144 ± 20 ka, likely rejuvenated periodically by later intrusions of juvenile magma. The exposed $\varepsilon_{Nd}(t) \approx -2$ syenites are chemically zoned, with a general increase in SiO_2 content from the lowest (57–62 wt%) to the highest (68 wt%) structural levels. Final crystallization of both the $\varepsilon_{Nd}(t) \approx -5$ and −2 magmas occurred at ~36.1 Ma, as reflected by the zircon U–Pb dates. The variations in U–Pb dates between different samples of the equigranular and inequigranular syenites suggest that different parts of the magma chamber cooled and crystallized at slightly different rates.

The largest differences between our revised model and Verplanck et al. (1999) are the origin of the $\varepsilon_{Nd}(t) \approx -5$ magmas and the relative timing of the $\varepsilon_{Nd}(t) \approx -5$ and −2 magmas. Verplanck et al. (1999) envisioned a single intrusion of $\varepsilon_{Nd}(t) \approx -2$ magma, followed by wall rock assimilation at the base of the pluton, which generated the $\varepsilon_{Nd}(t) \approx -5$ magma. The $\varepsilon_{Nd}(t) \approx -5$ magma then differentiated and moved up the sides of the $\varepsilon_{Nd}(t) \approx -2$ magma to form the AFG cupolas. The U–Pb dates presented here show that the Organ Needle pluton crystallized after eruption/crystallization of the Achenback Park tuff, Squaw Mountain tuff, and AFG. These data do not preclude the Verplanck et al. (1999) model; however, we prefer the interpretation that the $\varepsilon_{Nd}(t) \approx -2$ core of the Organ Needle pluton represents younger magmas that underplated an existing $\varepsilon_{Nd}(t) \approx -5$ magma chamber/mush zone. The later intrusion of $\varepsilon_{Nd}(t) \approx -2$ magmas may have triggered the tuff eruptions and kept the intrusive system partially molten for tens to hundreds of thousands of years. We suggest that the $\varepsilon_{Nd}(t) \approx -5$ magma was generated by partial melting of the lower crust, which could account for the consistent intrusion of $\varepsilon_{Nd}(t) \approx -5$ magmas over ≥2.4 Ma of magmatism in the Organ Mountains system.

Summary and conclusions

New high-precision U–Pb zircon dates provide precise constraints on the timing of volcanism and plutonism in the well-studied Organ Mountains caldera and batholith. The Cueva Tuff, Achenback Park tuff, and Squaw Mountain tuff erupted at 36.441 ± 0.020, 36.259 ± 0.016 and 36.215 ± 0.016 Ma, respectively. An alkali feldspar granite, which is chemically similar to the erupted tuffs, yielded a weighted mean $^{206}Pb/^{238}U$ date of 36.259 ± 0.021 Ma, synchronous with the eruption of the Achenback Park tuff. Weighted mean $^{206}Pb/^{238}U$ dates from the larger syenitic phase of the underlying Organ Needle pluton range from 36.130 ± 0.031 to 36.071 ± 0.012 Ma, and the youngest sample is 144 ± 20 to 188 ± 20 ka younger than the Squaw Mountain tuff and the central alkali feldspar granite/Achenback Park tuff, respectively. The dated samples come from both the $\varepsilon_{Nd}(t) \approx -5$ and $\varepsilon_{Nd}(t) \approx -2$ phases of the syenites and suggest that the two phases were comagmatic. Syenite and alkali feldspar granite exposures from the mapped northern extent of the Organ Needle pluton yielded significantly younger dates of 35.184 ± 0.020 to 35.032 ± 0.070 Ma, suggesting these units formed from a later magmatic pulse. The granite of Granite Peak and Sugarloaf Peak quartz monzonite also postdate formation of the Organ Needle pluton, with dates of 35.726 ± 0.016 and ≤34.051 ± 0.029 Ma, respectively.

Existing geochemical data and the new U–Pb dates are consistent with crystallization of the Organ Needle pluton and alkali feldspar granite, and eruption of the Achenback Park and Squaw Mountain tuffs, from a long-lived magma chamber/mush zone. In this model, a silicic precursor magma with $\varepsilon_{Nd}(t) \approx -2$ intruded and partially melted the lower continental crust, generating silicic $\varepsilon_{Nd}(t) \approx -5$ partial melts. The $\varepsilon_{Nd}(t) \approx -5$ magma rose into the upper crust where it underwent chemical differentiation. Underplating of fresh $\varepsilon_{Nd}(t) \approx -2$ magma rejuvenated the $\varepsilon_{Nd}(t) \approx -5$ mush zone, triggering eruption of tuff units. The intrusive magma then underwent protracted cooling and crystallization, with episodic recharge of $\varepsilon_{Nd}(t) \approx -2$ magmas, over a period of 144 ± 20 ka. Magmatic fluxes into the system for this model are ≥0.002 km^3/year. The proposed model suggests a close genetic link between plutonism and volcanism in small- to intermediate-sized caldera systems. Similarities between the Organ Mountains system and the Never Summer magmatic system, Colorado, suggest that the type of petrogenetic evolution envisioned here may be common to many small-volume silicic volcanic centers.

Acknowledgments We thank Bill Seager for useful discussions and accompanying Rioux in the field. His work on the Organ Mountains remains the basis for all subsequent studies. We thank Frank Spera for useful discussions of the data and ideas presented here. We thank

Jessica Creveling and Linnea Koons for carrying out mineral separations at MIT, Josh Garber for assistance with ArcMap, and Andrew Kylander Clark for assistance measuring the whole-rock Th/U of WSL-1. The Orejon Andesite was collected and originally dated by laser ablation-inductively coupled plasma-mass spectrometry (LA–ICP–MS) by Gabriela St. Pierre for an undergraduate research project at NMSU. Brian Knight, Conservation Branch Chief, Environmental Division, Fort Bliss, granted permission to Amato to sample on Fort Bliss property. Jeff and Julie Kester allowed sampling of volcanic rocks on their private land. Matt Zimmerer, assisted by David Winnett of Fort Bliss, collected and provided the samples analyzed at UNC. Finally, we appreciate the assistance of the undergraduate research assistants in the UNC Geochronology and Isotope Geochemistry Laboratory. We thank two anonymous reviewers for detailed suggestions that improved the manuscript. Any use of trade, product, or firm names is for descriptive purposes only and does not imply endorsement by the U.S. Government.

Funding The research and analyses at UNC were supported by a grant from the National Science Foundation (EAR-1050215).

Compliance with ethical standards

Conflict of interest The authors declare that they have no conflict of interest.

References

Annen C (2009) From plutons to magma chambers: thermal constraints on the accumulation of eruptible silicic magma in the upper crust. Earth Planet Sci Lett 284(3–4):409–416

Bachmann O, Bergantz GW (2004) On the origin of crystal-poor rhyolites: extracted from batholithic crystal mushes. J Petrol 45(8):1565–1582

Bachmann O, Bergantz GW (2008a) Deciphering magma chamber dynamics from styles of compositional zoning in large silicic ash flow sheets. Rev Mineral Geochem 69(1):651–674

Bachmann O, Bergantz GW (2008b) Rhyolites and their source mushes across tectonic settings. J Petrol 49(12):2277–2285

Bachmann O, Miller CF, de Silva SL (2007) The volcanic–plutonic connection as a stage for understanding crustal magmatism. J Volcanol Geoth Res 167(1–4):1–23

Bowring JF, McLean NM, Bowring SA (2011) Engineering cyber infrastructure for U-Pb geochronology: tripoli and U-Pb_Redux. Geochem Geophys Geosyst 12:Q0AA19

Brown SJA, Fletcher IR (1999) SHRIMP U-Pb dating of the preeruption growth history of zircons from the 340 ka Whakamaru Ignimbrite, New Zealand: evidence for > 250 k.y. magma residence times. Geology 27(11):1035–1038

Butcher D (1990) Geochemistry and Nd Sr Systematics of selected lithologic units of the Oligocene organ cauldron and batholith, South Central New Mexico, M.S.: New Mexico State University, p 145

Cather SM, Johnson BD, Mexico N (1984) Eocene tectonics and depositional setting of west-central New Mexico and eastern Arizona, New Mexico Bureau of Mines and Mineral Resources, New Mexico Institute of Mining and Technology, New Mexico Bureau of Mines and Mineral Resources Circular, p 192

Cooper KM, Kent AJR (2014) Rapid remobilization of magmatic crystals kept in cold storage. Nature 506(7489):480–483

Cooper KM, Reid MR (2008) Uranium-series crystal ages. Rev Mineral Geochem 69(1):479–544

Davis DW, Gray J, Gumming GL, Baadsgaard H (1977) Determination of the ^{87}Rb decay constant. Geochim Cosmochim Acta 41(12):1745–1749

Davis J, Coleman D, Gracely J, Gaschnig R, Stearns M (2012) Magma accumulation rates and thermal histories of plutons of the Sierra Nevada batholith. CA. Contri Mineral Petrol 163(3):449–465

Gelman SE, Gutiérrez FJ, Bachmann O (2013) On the longevity of large upper crustal silicic magma reservoirs. Geology. doi:10.1130/G34241.1

Glazner AF, Bartley JM, Coleman DS, Gray W, Taylor RZ (2004) Are plutons assembled over millions of years by amalgamation from small magma chambers? GSA Today 14(4/5):4–12

Halliday AN, Davidson JP, Hildreth W, Holden P (1991) Modelling the petrogenesis of high Rb/Sr silicic magmas. Chem Geol 92(1–3):107–114

Hildreth W (1981) Gradients in silicic magma chambers: implications for lithospheric magmatism. Journal of Geophysical Research: Solid Earth 86(B11):10153–10192

Hildreth W (2004) Volcanological perspectives on long valley, mammoth mountain, and mono craters: several contiguous but discrete systems. J Volcanol Geoth Res 136(3–4):169–198

Ickert RB (2013) Algorithms for estimating uncertainties in initial radiogenic isotope ratios and model ages. Chem Geol 340:131–138

Jacob K, Farmer GL, Buchwaldt R, Bowring S (2015) Deep crustal anatexis, magma mixing, and the generation of epizonal plutons in the Southern Rocky Mountains, Colorado. Contrib Miner Petrol 169(1):1–23

Jaffey AH, Flynn KF, LE Glendenin, Bentley WC, Essling AM (1971) Precision measurement of half-lives and specific activities of ^{235}U and ^{238}U. Phys Rev C 4(5):1889–1906

Kuiper KF, Deino A, Hilgen FJ, Krijgsman W, Renne PR, Wijbrans JR (2008) Synchronizing rock clocks of earth history. Science 320(5875):500–504

Lipman PW (1984) The roots of ash flow calderas in western North America: windows into the tops of granitic batholiths. J Geophys Res Solid Earth 89(B10):8801–8841

Lipman PW (2007) Incremental assembly and prolonged consolidation of cordilleran magma chambers: evidence from the Southern Rocky Mountain volcanic field. Geosphere 3(1):42–70

Lipman PW, Bachmann O (2015) Ignimbrites to batholiths: integrating perspectives from geological, geophysical, and geochronological data. Geosphere 11(3):705–743

Loring AK, Loring RB (1980) K/Ar ages of middle Tertiary igneous rocks from southern New Mexico. Isochron/West 28:17–19

Lugmair GW, Marti K (1978) Lunar initial ^{143}Nd/^{144}Nd: differential evolution of the lunar crust and mantle. Earth Planet Sci Lett 39(3):349–357

Mack G, Kottlowski F, Seager W (1998) The stratigraphy of south-central New Mexico, In: Proceedings Las Cruces country II: New Mexico Geol. Soc. 49th Ann. Field Conf. Guidebook, pp 135–154

Mattinson JM (2005) Zircon U/Pb chemical abrasion (CA-TIMS) method; combined annealing and multi-step partial dissolution analysis for improved precision and accuracy of zircon ages. Chem Geol 220(1–2):47–66

Matzel JEP, Bowring SA, Miller RB (2006) Time scales of pluton construction at differing crustal levels: examples from the Mount Stuart and Tenpeak intrusions, North Cascades, Washington. Geol Soc Am Bull 118(11–12):1412–1430

McIntosh W, Sutter J, Chapin C, Kedzie L (1990) High-precision ^{40}Ar/^{39}Ar sanidine geochronology of ignimbrites in the Mogollon-Datil volcanic field, southwestern New Mexico. Bull Volc 52(8):584–601

McLean NM, Bowring JF, Bowring SA (2011) An algorithm for U-Pb isotope dilution data reduction and uncertainty propagation. Geochem Geophys Geosyst 12:Q0AA18

McMillan NJ (2004) Magmatic record of Laramide subduction and the transition to Tertiary extension: Upper Cretaceous through Eocene igneous rocks of New Mexico, In Mack GH, Giles KA (eds.), The geology of New Mexico: a geologic history, Volume 11

McMillan NJ, Dickin AP, Haag D (2000) Evolution of magma source regions in the Rio Grande rift, southern New Mexico. Geol Soc Am Bull 112(10):1582–1593

Metcalf RV (2004) Volcanic-plutonic links, plutons as magma chambers and crust-mantle interaction: a lithospheric scale view of magma systems. Geol Soc Am Spec Papers 389:357–374

Mills R, Coleman D (2013) Temporal and chemical connections between plutons and ignimbrites from the Mount Princeton magmatic center. Contrib Miner Petrol 165(5):961–980

Min K, Mundil R, Renne PR, Ludwig KR (2000) A test for systematic errors in $^{40}Ar/^{39}Ar$ geochronology through comparison with U/Pb analysis of a 1.1-Ga rhyolite. Geochim Cosmochim Acta 64(1):73–98

Reid MR (2014) Timescales of Magma Transfer and Storage in the Crust. In: Rudnick RL (ed) Treatise on geochemistry, 2nd edn. Elsevier, Oxford, pp 181–201

Reid MR, Coath CD, Mark Harrison T, McKeegan KD (1997) Prolonged residence times for the youngest rhyolites associated with Long Valley Caldera:^{230}Th—^{238}U ion microprobe dating of young zircons. Earth Planet Sci Lett 150(1–2):27–39

Schoene B, Schaltegger U, Brack P, Latkoczy C, Stracke A, Günther D (2012) Rates of magma differentiation and emplacement in a ballooning pluton recorded by U-Pb TIMS-TEA, Adamello batholith, Italy. Earth Planet Sci Lett 355–356:162–173

Seager WR (1981) Geology of organ mountains and southern San Andres mountains, New Mexico, New Mexico Bureau of Mines and Mineral Resources Memoir 36, p 97

Seager WR, McCurry M (1988) The cogenetic organ cauldron and batholith, south central New Mexico: evolution of a large-volume ash flow cauldron and its source magma chamber. J Geophys Res Solid Earth 93(B5):4421–4433

Simon JI, Renne PR, Mundil R (2008) Implications of pre-eruptive magmatic histories of zircons for U-Pb geochronology of silicic extrusions. Earth Planet Sci Lett 266(1–2):182–194

Smith RL (1979) Ash-flow magmatism. Geol Soc Am Spec Papers 180:5–28

Tappa MJ, Coleman DS, Mills RD, Samperton KM (2011) The plutonic record of a silicic ignimbrite from the Latir volcanic field, New Mexico. Geochem Geophys Geosyst 12(10):Q10011

Vazquez JA, Lidzbarski MI (2012) High-resolution tephrochronology of the Wilson Creek Formation (Mono Lake, California) and Laschamp event using ^{238}U-^{230}Th SIMS dating of accessory mineral rims. Earth Planet Sci Lett 357–358:54–67

Vazquez J, Reid M (2002) Time scales of magma storage and differentiation of voluminous high-silica rhyolites at Yellowstone caldera, Wyoming. Contri Mineral Petrol 144(3):274–285

Verplanck PL (1996) Origin of a compositionally-zoned, epizonal magma body; a detailed geochemical study of the Organ Needle Pluton, south-central New Mexico (Ph.D.), University of Colorado, p 296

Verplanck PL, Farmer GL, McCurry M, Mertzman S, Snee LW (1995) Isotopic evidence on the origin of compositional layering in an epizonal magma body. Earth Planet Sci Lett 136(1–2):31–41

Verplanck PL, Farmer GL, McCurry M, Mertzman SA (1999) The chemical and isotopic differentiation of an epizonal magma body: organ needle pluton, New Mexico. J Petrol 40(4):653–678

Watson EB, Harrison TM (1983) Zircon saturation revisited: temperature and composition effects in a variety of crustal magma types. Earth Planet Sci Lett 64(2):295–304

Zimmerer MJ, McIntosh WC (2013) Geochronologic evidence of upper-crustal in situ differentiation: silicic magmatism at the Organ caldera complex, New Mexico. Geosphere 9(1):155–169